

**UNSTEADY MHD HEAT AND MASS TRANSFER OVER AN INFINITE  
POROUS FLAT PLATE WITH CONVECTIVE SURFACE BOUNDARY  
CONDITIONS**

**BY**

**ODERO ISAIAH OTIENO**

**A THESIS SUBMITTED IN FULFILLMENT OF THE REQUIREMENTS  
FOR THE DEGREE OF DOCTOR OF PHILOSOPHY**

**SCHOOL OF MATHEMATICS, STATISTICS AND ACTUARIAL  
SCIENCE**

**MASENO UNIVERSITY**

**©2018**



## DECLARATION

This thesis is my own work and has not been presented for a degree award in any other institution.

Signature: \_\_\_\_\_

Date: \_\_\_\_\_

Odero, Isaiah Otieno,  
PG/PHD/00026/2012

This thesis has been submitted for examination with our approval as the university supervisors

Signature: \_\_\_\_\_

Date: \_\_\_\_\_

Prof. A. W. Manyonge  
Maseno University, Kenya.

Signature: \_\_\_\_\_

Date: \_\_\_\_\_

Prof. J. K. Bitok  
University of Eldoret, Kenya.

## ACKNOWLEDGEMENT

Any scientific investigation results in the accumulation of debts to those who have given their time to help in research work and dig through their files for documents. Without exception of those I have approached for specific pieces of information have been generous with their time and enthusiastic to support this study. First of all, I would like to thank the Almighty God for His love, favour and divine provision to me.

My sincere gratitude goes to my supervisor, Professor Alfred W. Manyonge for his guidance, encouragement, useful insight and valuable comments during the supervision. Thank you so much *A.M* for all your effort in my academic development. I would also wish to thank my second supervisor Professor Jacob K. Bitok for his guidance and encouragement during the period of my study that made this work a success.

I wish to heartily thank the organizing secretary ICAFD - 2012, Professor J. Prakash of the University of Botswana for sponsoring me to have research proposal presented and discussed during the 27-28 September, 2012 University of Botswana conference. I also wish to express my appreciation to the staff of School of Mathematics of Maseno University for their support and encouragement.

Special thanks also go to my dear wife, Loice, daughter Sheryle, sons Georges and Damian. May Almighty God bless you for supporting me. I am forever indebted to my mother Wilcister Odero and my late dad George Odero who sacrificed a lot to educate me. To my sister Benter and brothers Benard and Peter, thank you for your love. Lastly to those who directly or indirectly contributed to the success of this research work and are not mentioned here, I say thank you and may the Almighty God reward you abundantly.

## DEDICATION

*To my parents, the late dad George Odero and mum Wilcister Odero*

*To my dear wife Loice*

*To my daughter Sheryle, sons Georges and Damian*

*To my siblings Benter, Peter and Benard.*

## ABSTRACT

Unsteady MHD heat and mass transfer over an infinite flat plate with convective surface boundary condition problems have received little attention yet they are of great importance in many scientific and engineering fields particularly in the manufacture and maintenance of ship propulsion unit and thermal energy storage processes in nuclear plants. Every research work that would give results aimed at improving the efficiency of the modern marine vessels is of significance to the fields of naval architecture and marine engineering. Past studies by various researchers in the field of MHD fluid flows seems to have ignored the effects of ion-slip and Hall currents on velocity, temperature and concentration profiles of fluid flow. In this research, unsteady MHD heat and mass transfer over an infinite flat porous plate with convective surface boundary conditions is studied and more specifically to investigate the contribution of the combined effects of ion-slip and Hall currents on the velocity, temperature and concentration of an incompressible, viscous and electrically conducting fluid subject to cooling and heating of the plate by free convective currents and constant heat flux. The objective of this study was to formulate and solve, using explicit finite difference scheme, the coupled partial differential equations of momentum, energy and concentration of species describing the flow. The flow equations were non-dimensionalized, transformed then programmed into a mathematica code and results generated in graphs. The effects of physical parameters on velocity, temperature and concentration fields are analyzed from graphs. Our analysis of the graphical results obtained shows that velocity and thermal boundary layer thickness increase with increase in ion-slip and Hall parameters for the cooling of the plate by free convection in the presence of constant heat flux. The thermal boundary layer thickness increases with cooling of the plate by free convection and presence of constant heat flux. The concentration of the fluid increases with increase in time or decrease in mass diffusion parameter or withdrawal of suction velocity. The results of this research can serve as prototype for practical propulsion type of problems, for example, generation of propulsion force in moving ship.

## TABLE OF CONTENTS

DECLARATION . . . . .	ii
ACKNOWLEDGEMENT . . . . .	iii
DEDICATION . . . . .	iv
ABSTRACT . . . . .	v
TABLE OF CONTENTS . . . . .	vi
LIST OF FIGURES . . . . .	vii
INDEX OF NOTATION . . . . .	x
<b>CHAPTER 1 INTRODUCTION . . . . .</b>	<b>1</b>
1.1 Preliminary concepts . . . . .	2
1.2 Statement of the problem . . . . .	7
1.3 Objectives of the study . . . . .	10
1.4 Significance of the study . . . . .	10
1.5 Research methodology . . . . .	11
<b>CHAPTER 2 LITERATURE REVIEW . . . . .</b>	<b>13</b>
2.1 MHD flows past infinite plates . . . . .	13
2.2 MHD free convection flows . . . . .	15
<b>CHAPTER 3 MATHEMATICAL FORMULATION . . . . .</b>	<b>19</b>
3.1 Problem setting . . . . .	19
3.2 Mathematical analysis . . . . .	21
<b>CHAPTER 4 MODEL SOLUTION . . . . .</b>	<b>29</b>
4.1 Numerical technique: . . . . .	29
4.2 Convergence and stability . . . . .	31
<b>CHAPTER 5 RESULTS AND DISCUSSION . . . . .</b>	<b>33</b>

5.1	Concentration profiles . . . . .	33
5.2	Temperature profiles . . . . .	33
5.3	Velocity profiles . . . . .	35
<b>CHAPTER 6 SUMMARY AND RECOMMENDATIONS . . . . .</b>		<b>43</b>
6.1	Summary . . . . .	43
6.2	Recommendations . . . . .	44
<b>REFERENCES . . . . .</b>		<b>45</b>
<b>APPENDICES . . . . .</b>		<b>49</b>
A.1	Mathematica code (Concentration) . . . . .	49
A.2	Mathematica code (Temperature) . . . . .	51
A.3	Mathematica code (Velocity) . . . . .	53

## LIST OF FIGURES

3.1	Flow configuration with the coordinate system . . . . .	20
4.1	Computational molecule for the explicit numerical difference scheme. . .	31
5.1	Concentration profiles for different values of $S_c$ when $v_0 = 0.5$ and $t = 0.032$ .	34
5.2	Concentration profiles for different values of $t$ when $S_c = 0.4$ and $v_0 = 0.5$ .	34
5.3	Concentration profiles for different values of $v_0$ when $S_c = 0.4$ and $t = 0.032$ .	34
5.4	Temperature profiles for different values of $\beta_n$ when $S_c = 0.4$ , $v_0 = 0.5$ , $G_r = 0.2$ , $G_c = 1.0$ , $P_r = 7.0$ , $E_c = 0.01$ , $t = 0.032$ , $\beta_m = 1.0$ , $M^2 = 5.0$ , $B_i = 1.0$ . . . . .	35
5.5	Temperature profiles for different values of $G_c$ when $S_c = 0.4$ , $v_0 = 0.5$ , $G_r = 0.2$ , $\beta_n = 0.2$ , $P_r = 7.0$ , $E_c = 0.01$ , $t = 0.032$ , $\beta_m = 1.0$ , $M^2 = 5.0$ , $B_i = 1.0$ . . . . .	36
5.6	Temperature profiles for different values of $\beta_m$ when $S_c = 0.4$ , $v_0 = 0.5$ , $G_r = 0.2$ , $\beta_n = 0.2$ , $P_r = 7.0$ , $E_c = 0.01$ , $t = 0.032$ , $G_c = 1.0$ , $M^2 = 5.0$ , $B_i = 1.0$ . . . . .	36
5.7	Temperature profiles for different values of $t$ when $S_c = 0.4$ , $v_0 = 0.5$ , $G_r = 0.2$ , $\beta_n = 0.2$ , $P_r = 7.0$ , $E_c = 0.01$ , $G_c = 1.0$ , $\beta_m = 1.0$ , $M^2 = 5.0$ , $B_i = 1.0$ . . . . .	37
5.8	Temperature profiles for different values of $v_0$ when $S_c = 0.4$ , $G_c = 1.0$ , $G_r = 0.2$ , $\beta_n = 0.2$ , $P_r = 7.0$ , $E_c = 0.01$ , $t = 0.032$ , $\beta_m = 1.0$ , $M^2 = 5.0$ , $B_i = 1.0$ . . . . .	37
5.9	Velocity profiles for different values of $\beta_m$ when $S_c = 0.4$ , $v_0 = 0.5$ , $G_r =$ $0.2$ , $G_c = 1.0$ , $P_r = 7.0$ , $E_c = 0.01$ , $t = 0.032$ , $\beta_n = 0.2$ , $M^2 = 5.0$ , $B_i = 1.0$	39
5.10	Velocity profiles for different values of $\beta_n$ when $S_c = 0.4$ , $v_0 = 0.5$ , $G_r =$ $0.2$ , $G_c = 1.0$ , $P_r = 7.0$ , $E_c = 0.01$ , $t = 0.032$ , $\beta_m = 1.0$ , $M^2 = 5.0$ , $B_i = 1.0$	39

5.11	Velocity profiles for different values of $\beta_m$ when $S_c = 0.4$ , $v_0 = 0.5$ , $G_r = -0.2$ , $G_c = 1.0$ , $P_r = 7.0$ , $E_c = 0.01$ , $t = 0.032$ , $\beta_n = 0.2$ , $M^2 = 5.0$ , $B_i = 1.0$	40
5.12	Velocity profiles for different values of $\beta_n$ when $S_c = 0.4$ , $v_0 = 0.5$ , $G_r = -0.2$ , $G_c = 1.0$ , $P_r = 7.0$ , $E_c = 0.01$ , $t = 0.032$ , $\beta_m = 1.0$ , $M^2 = 5.0$ , $B_i = 1.0$	40
5.13	Velocity profiles for different values of $M^2$ when $S_c = 0.4$ , $v_0 = 0.5$ , $G_r = 0.2$ , $G_c = 1.0$ , $P_r = 7.0$ , $E_c = 0.01$ , $t = 0.032$ , $\beta_m = 1.0$ , $\beta_n = 0.2$ , $B_i = 1.0$	41
5.14	Velocity profiles for different values of $G_c$ when $S_c = 0.4$ , $v_0 = 0.5$ , $G_r = 0.2$ , $M^2 = 5.0$ , $P_r = 7.0$ , $E_c = 0.01$ , $t = 0.032$ , $\beta_m = 1.0$ , $\beta_n = 0.2$ , $B_i = 1.0$	41
5.15	Velocity profiles for different values of $v_0$ when $S_c = 0.4$ , $G_c = 1.0$ , $G_r = 0.2$ , $M^2 = 5.0$ , $P_r = 7.0$ , $E_c = 0.01$ , $t = 0.032$ , $\beta_m = 1.0$ , $\beta_n = 0.2$ , $B_i = 1.0$	41
5.16	Velocity profiles for different values of $t$ when $S_c = 0.4$ , $G_c = 1.0$ , $G_r = 0.2$ , $M^2 = 5.0$ , $P_r = 7.0$ , $E_c = 0.01$ , $v_0 = 0.5$ , $\beta_m = 1.0$ , $\beta_n = 0.2$ , $B_i = 1.0$	42

## INDEX OF NOTATIONS

<p>MHD    Magnetohydrodynamic . . . . . 1</p> <p><b>V</b>    Velocity vector . . . . . 1</p> <p><b>B</b>    Magnetic field intensity . . . . . 1</p> <p><b>J</b>    Current density vector . . . . . 1</p> <p><math>x_1, y_1, z_1</math>    Dimensional Cartesian co-ordinates . . . . . 3</p> <p><math>u_1, v_1, w_1</math>    Dimensional velocity components of <b>V</b> . . . . . 3</p> <p><math>\tau</math>    Shear stress . . . . . 3</p> <p><math>\mu</math>    Coefficient of dynamic viscosity . . . . . 3</p> <p><math>\rho</math>    Fluid density . . . . . 4</p> <p><math>t_1</math>    Dimensional time . . . . . 4</p> <p><math>\mathbf{f}_B</math>    Body force per unit mass . . . . . 4</p> <p><b>g</b>    Gravitational field strength vector . . . . . 5</p> <p><math>C_p</math>    Specific heat capacity at constant pressure . . . . . 5</p> <p><b>Q</b>    Internal heat generation . . . . . 5</p> <p><b>K</b>    Thermal conductivity . . . . . 5</p> <p><math>\phi</math>    Thermal energy due to dissipation of heat . . . . . 5</p> <p><b>T</b>    Dimensional temperature . . . . . 5</p> <p><math>\sigma</math>    Electric conductivity . . . . . 5</p> <p><math>\mu_0</math>    Permeability of free space . . . . . 5</p> <p><math>\epsilon_0</math>    Permittivity of free space . . . . . 5</p>	<p><b>E</b>    Electric field intensity vector . . . . . 6</p> <p><b>e</b>    Unit electric charge . . . . . 6</p> <p><math>\mathbf{F}_e</math>    Force on electric charge . . . . . 6</p> <p><math>\rho_e</math>    Electric charge density . . . . . 6</p> <p><math>B_0</math>    magnetic field vector applied to the plate . . . . . 6</p> <p>e.m.f    Electromotive force . . . . . 6</p> <p><b>U</b>    Velocity of the plate . . . . . 8</p> <p><math>C_1</math>    Dimensional concentration of the injected material . . . . . 8</p> <p><b>P</b>    Pressure . . . . . 8</p> <p><b>q</b>    Heat flux vector . . . . . 9</p> <p><b>D</b>    Diffusion coefficient . . . . . 10</p> <p><math>v_0^*</math>    Dimensional suction velocity . . . . . 19</p> <p><math>(f_B)_{x_1}</math>    Component of the body force along <math>x_1</math> -axis . . . . . 20</p> <p><math>(f_B)_{y_1}</math>    Component of the body force along <math>y_1</math> -axis . . . . . 20</p> <p><math>(f_B)_{z_1}</math>    Component of the body force along <math>z_1</math> -axis . . . . . 20</p> <p><math>J_{x_1}, J_{y_1}, J_{z_1}</math>    Components of current density vector, <b>J</b> . . . . . 21</p> <p><math>\beta_c</math>    Coefficient of volumetric expansion due to concentration gradient . . . . . 21</p>
---	---

$C_\infty$	Dimensional free stream concentration . . . . .	21	$B_i$	Convective heat exchange parameter . . . . .	26
$\beta_T$	Coefficient of volumetric expansion due to temperature	21	$E_c$	Eckert number . . . . .	26
$B_{x_1}, B_{y_1}, B_{z_1}$	Components of magnetic field vector, $\mathbf{B}$ . . . . .	23	$S_c$	Schmidt number . . . . .	27
$E_{x_1}, E_{y_1}, E_{z_1}$	Components of electric field vector, $\mathbf{E}$ . . . . .	23	$Z$	Complex velocity . . . . .	27
$\omega_e$	Cyclotron frequency . . . . .	24	$\bar{Z}$	Complex conjugate of $Z$ . . . . .	27
$\tau_e$	Electron collision time . . . . .	24	$k'$	Coefficient of heat diffusivity . . . . .	32
$\beta_n$	Ion slip parameter . . . . .	24	$\lambda$	Mesh ratio parameter . . . . .	32
$\beta_m$	Hall current parameter . . . . .	24			
$u, v, w$	Dimensionless velocity components . . . . .	25			
$v_0$	Dimensionless suction velocity	25			
$t$	Dimensionless time . . . . .	25			
$C_w$	Concentration of injected material at the plate wall . . . . .	25			
$C$	Dimensionless concentration of the the injected material . . . . .	25			
$\nu$	Coefficient of kinematic viscosity	25			
$\theta$	Dimensionless temperature . . . . .	25			
$G_r$	Grashof number . . . . .	26			
$G_c$	Modified Grashof number . . . . .	26			
$M$	Magnetic parameter . . . . .	26			
$P_r$	Prandtl number . . . . .	26			

# CHAPTER 1

## INTRODUCTION

The word Magnetohydrodynamics (MHD) refers to the branch of fluid mechanics which is concerned with the interaction of electrically conducting fluids and electromagnetic fields. Some of these fluids are mercury, salty water, molten iron, ionized gases (plasma) e.g solar atmosphere. The official birth of incompressible fluid magnetohydrodynamics was in 1937 when Hartman and Lazarus [1] performed theoretical and experimental studies of MHD flows in ducts using mercury. It was observed that a force is produced on the fluid in the direction normal to both the applied electric and magnetic fields. Later, a Swedish electrical engineer Alfvén [2] in 1947 from his research on magnetohydrodynamics described astrophysical phenomenon as an independent scientific discipline. Thereafter several others [3, 4, 10, 16, 25, 28] have continued to conduct research into various aspects of the problem of MHD flows with respect to application. In many engineering practical applications, the knowledge of MHD is very useful as it has been used to explain certain phenomena in the universe [2, 13]. This has led to intensive scientific research in the field of computational modeling of MHD fluid flows [31, 33]. MHD covers phenomena in electrically conducting fluid where the velocity of the fluid,  $\mathbf{V}$ , and the magnetic field intensity,  $\mathbf{B}$ , are coupled. Any movement of a conducting material in a magnetic field, and electric field with currents,  $\mathbf{J}$ , experiences MHD force given by  $\mathbf{J} \times \mathbf{B}$ , known as the Lorentz force [1]. When a viscous electrically conducting liquid flows in the presence of a transverse magnetic field, electromagnetic forces such as the Lorentz force acts on the fluid particles thereby altering the geometry of their motion. This motion of the particles creates viscous dissipation in the fluid which affects the overall motion of the fluid. A wide variety of problems dealing with heat and fluid flow over porous and non-porous surfaces have been studied with both Newtonian and non-Newtonian fluids and with the inclusion of imposed magnetic fields and power law variation of the velocity [8, 18, 32]. MHD boundary layer with heat and mass transfer past vertical plates are found in

many engineering and geophysical applications such as geothermal reservoirs and thermal insulation [4, 27]. It is also reported that heat and mass transfer occur in processes, such as drying evaporation at the surface of water body and energy distribution of temperature and moisture over agricultural fields [17, 26]. Several interesting computational studies of steady MHD boundary layer flows with heat and mass transfer have appeared in recent years [3, 17, 19, 33]. The idea of using convective boundary condition was recently introduced by Aziz [3] in 2009 to study the classical boundary layer flow over a flat surface. Convective boundary condition has been found to be more general and realistic especially with respect to several engineering and industrial processes like transpiration cooling processes as explained by Singh [5]. Convective heat transfer studies are very important since it has been found to be very useful in processes involving high temperatures such as thermal energy storage and heat exchange design [11, 29, 32]. Some researchers [17, 33] have also showed that the use of some polymer fluids like polyethylene oxide solution which have better electromagnetic properties, can be used as a cooling liquid as their flow can be regulated by external magnetic fields in order to improve the quality of final product. In this study, our work is to modify the study of Aziz [3] who researched on steady MHD thermal boundary layer flow and demonstrated that a similarity solution is only possible if the convective heat transfer associated with the hot fluid on the lower surface of the plate is proportional to  $x^{-\frac{1}{2}}$ . His results showed that for a constant heat flux, Representative Prandtl numbers of 0.1 - 0.72 or 7.0- 10.0 for computations can be carried out for air or water respectively. We therefore carry out a study on unsteady MHD mass and heat flow for a thermal, velocity and solutal boundary layers subject to convective surface boundary condition.

## **1.1 Preliminary concepts**

In this section, we give some basic definitions that are vital in this study.

### **Definition 1.1.0.1. Laminar flow**

Laminar flow sometimes known as streamline flow is one in which all fluid particles at

the same distance from the axis of a plate would have the same velocity so that the fluid could be thought of as moving in layers. That is, the paths taken by the individual fluid particles do not cross one another.

**Definition 1.1.0.2. Two dimensional flow**

Is a fluid flow in which the motion pattern in a certain plane is the same as that in all other planes within the fluid. For example, in rectangular coordinate system, the velocity is a function of time and the two rectangular space coordinates.

Mathematically, if  $u_1$  and  $v_1$  are the  $x_1$  and the  $y_1$  velocity components of the velocity,  $\mathbf{V}$ , respectively, then [36].

$$u_1 = f_1(x_1, y_1), v_1 = f_2(x_1, y_1) \tag{1.1}$$

where  $f_1$  and  $f_2$  in Equation (1.1) are arbitrary functions of  $x_1$  and  $y_1$ .

**Definition 1.1.0.3. Unsteady flow**

This is a type of flow in which the fluid flow variables change with time. For this study, fluid flow variables such as velocity, temperature and concentration of the fluid at a point in the flow region change with time. Otherwise the fluid flow is said to be steady.

**Definition 1.1.0.4. Viscosity and viscous dissipation**

Viscosity is the property of a fluid which determines its resistance to shearing stresses between the layers of the fluid. It is a measure of the internal fluid friction which causes resistance to the fluid flow.

Mathematically,

$$\tau = \mu \frac{du_1}{dy_1} \tag{1.2}$$

where  $\tau$  is the shear stress,  $\mu$  is the coefficient of dynamic viscosity and  $\frac{du_1}{dy_1}$  is the velocity gradient. Fluids which follow the relation defined in equation (1.2) are referred to as Newtonian fluids as explained by Chandra [34].

When an electrically conducting fluid flows, an increase in temperature leads to an increase in its skin friction or viscosity. This viscosity increase could be along the x-axis, y-axis or z-axis as explained by Manyonge [36]. This phenomenon is called viscous dissipation.

**Definition 1.1.0.5. Equation of continuity**

If  $\mathbf{V}$  is the velocity of the fluid whose density is  $\rho$ , [34, 36] then

$$\frac{\partial \rho}{\partial t_1} + \nabla \cdot (\rho \mathbf{V}) = 0 \quad (1.3)$$

Where  $\nabla$  is the gradient operator. Equation (1.3) means that mass is conserved and that for any liquid, the flow is assumed to be continuous, that is, no empty spaces occur between particles which are in contact.

**Definition 1.1.0.6. Equation of momentum**

The equation of momentum also referred to as Navier-Stokes equation of fluid motion (with the Lorentz force) as described by Crank [35] is given by

$$\rho \left( \frac{\partial \mathbf{V}}{\partial t_1} + (\mathbf{V} \cdot \nabla) \mathbf{V} \right) = -\nabla P + \mu \nabla^2 \mathbf{V} + \rho \mathbf{f}_B \quad (1.4)$$

where  $\mathbf{f}_B$  and  $P$  in equation (1.4) are the body force per unit mass and pressure of the fluid respectively.  $\mathbf{f}_B$  is given by

$$\mathbf{f}_B = \mathbf{g} + \mathbf{J} \times \mathbf{B} \quad (1.5)$$

where  $\mathbf{g}$ ,  $\mathbf{J}$ ,  $\mathbf{B}$  in equation (1.5) are the gravitational field strength, current density and magnetic field vectors respectively.

**Definition 1.1.0.7. Equation of energy**

Equation of energy with joule heating [34, 36] is given by

$$\rho C_p \left( \frac{\partial T}{\partial t_1} + (\mathbf{V} \cdot \nabla) T \right) = k \nabla^2 T + \mu \phi + Q + \frac{\mathbf{J}^2}{\sigma} \quad (1.6)$$

where  $C_p, k, T, \sigma, \phi$  and  $Q$  in equation (1.6) are the specific heat capacity at constant pressure, thermal conductivity of the fluid, temperature of the fluid, electric conductivity of the fluid and the thermal energy due to dissipation of heat and internal heat generation respectively.

**Definition 1.1.0.8. Maxwell's equations**

The basic law of electricity and magnetism can be summarized in form of differential equations form. The equations provide link between the electric and magnetic fields independent of the properties of matter [1, 36, 38]. The set of Maxwell's electromagnetic differential equations that considers the fact that most hydromagnetic flows are unsteady is given by;

i) Faraday's law of induction: The voltage induced in a closed circuit is proportional to the rate of change of the magnetic flux it encloses.

$$-\frac{\partial \mathbf{B}}{\partial t_1} = \nabla \times \mathbf{E} \tag{1.7}$$

ii) Amperé's circuital law: The magnetic field induced around a closed loop is proportional to the electric current plus rate of change of electric field it encloses.

$$\nabla \times \mathbf{B} = \mu_0 \left( \mathbf{J} + \epsilon_0 \frac{\partial \mathbf{E}}{\partial t_1} \right) \tag{1.8}$$

Assuming permeability of free space,  $\mu_0$  and permittivity of free space,  $\epsilon_0$  are both unity, then Amperé's circuital law described in equation (1.8) reduces to:

$$\nabla \times \mathbf{B} = \mathbf{J} + \frac{\partial \mathbf{E}}{\partial t_1} \tag{1.9}$$

iii) Gauss's law: The electric flux leaving a volume is proportional to the charge inside.

$$\nabla \cdot \mathbf{E} = \rho_e \tag{1.10}$$

vi) Gauss's law for magnetism: There are no magnetic monopoles; that is total magnetic flux through a closed surface is zero.

$$\nabla \cdot \mathbf{B} = 0 \quad (1.11)$$

where  $\mathbf{B}$  in equations (1.9) and (1.11) is the magnetic field intensity,  $\mathbf{E}$  is the electric field intensity,  $\mathbf{J}$  in equation (1.9) is the current density.

**Definition 1.1.0.9. Ohm's law**

An electric charge,  $e$ , moving in an electromagnetic field encounters an electric force,  $\mathbf{V} \times \mathbf{B}$ . The resultant force,  $\mathbf{F}_e$ , on the charge is given by the Lorenz's equation [2, 34] which is expressed as

$$\mathbf{F}_e = \mathbf{E} + \mathbf{V} \times \mathbf{B} \quad (1.12)$$

In MHD fluid flow, this force acts on the fluid particles and in the direction normal to both  $\mathbf{J}$  and  $\mathbf{B}$ . The generalized Ohm's law is given by.

$$\mathbf{J} = \sigma(\mathbf{E} + \mathbf{V} \times \mathbf{B}) + \rho_e \mathbf{V} \quad (1.13)$$

where the term  $\rho_e \mathbf{V}$  in equation (1.13) represents the displacement current usually negligible at any fluid velocity  $\mathbf{V}$  if the magnetic field associated with electric field everywhere in the flow does not vary as is our case since  $B_0$ , which is the magnetic field vector applied to the plate is constant and  $\sigma$  is the electric conductivity. The law reduces to

$$\mathbf{J} = \sigma(\mathbf{E} + \mathbf{V} \times \mathbf{B}) \quad (1.14)$$

**Definition 1.1.0.10. Hall effect**

An electromotive force (e.m.f) is always set up transversally or across a current carrying conductor when a perpendicular magnetic field is applied on the conductor [1, 2]. This phenomenon called Hall effect has always been used in the determination of flux density,

$\mathbf{B}$ , of a magnetic field.

**Definition 1.1.0.11. Free convection**

In a free convection flow, as discussed by Kinyanjui [30], the fluid motion is as result of density gradient due to either temperature or concentration variation.

**Definition 1.1.0.12. Convective heat transfer**

Convective heat transfer involves heat energy exchange between boundary surfaces and an adjacent fluid due to temperature variation [31, 34, 36].

**Definition 1.1.0.13. Convective mass transfer**

This involves the transport of materials (e.g chemical ions) between boundary surface and moving fluid [17, 21, 33]. Mass transport always play an important role in many industrial processes, for example, the removal of pollutants from plant discharge.

**Definition 1.1.0.14. Convective boundary condition**

Here the exchange of heat takes place between the surface or boundary and the surrounding environment due temperature gradient in the fluid [3, 4, 30]. Convective boundary condition assumes that heat conduction at the surface of a boundary is equal to the heat convection at the surface in the same direction.

**Definition 1.1.0.15. Dimensionless quantity**

It is a quantity without any physical unit(s) and therefore is treated as just a pure number. A quantity with physical unit(s) is referred to as dimensioned or dimensional quantity, for instance force is a dimensioned quantity having unit as newton(N).

## **1.2 Statement of the problem**

The magnetohydrodynamics (MHD) flow over an infinite plate is a classical problem that has applications in MHD power generators, MHD pumps where MHD principle is used in pumping of materials that are hard to pump using conventional pumps and propulsion type of problems in propulsion units in ships. Heat and mass transfer occur in processes

such as drying, evaporation at the surface of a water body, and energy transfer in a wet cooling tower. Numerous research work concerning the MHD flows have been obtained under different physical effects. In all cases, the Hall current and ion-slip current terms were assumed to be negligible, hence ignored in applying Ohms's law as they have no marked effect for small and moderate values of the magnetic field. However, the trend for the application of MHD is towards a strong magnetic field, so that the influence of electromagnetic field is noticeable. Under these conditions, the ion-slip and Hall currents have a marked effect on the magnitude and direction of the current density and magnetic force term and consequently on the velocity and temperature profiles of MHD fluid flows. Therefore, we carried out a research on the combined effects of ion-slip current and Hall current on the unsteady MHD mass and heat transfer flow over an infinite horizontal porous plate with convective surface boundary condition so as find out how velocity, temperature and concentration profiles vary with different values of thermo-physical parameters. We consider an unsteady MHD heat and mass transfer for an incompressible, viscous and electrically conducting fluid over a moving infinite porous flat plate with convective surface boundary condition. The plate is taken to be electrically non-conducting and is along the  $x_1$ -axis. A uniform transverse magnetic field  $B_0$  is applied perpendicularly to the  $x_1z_1$ - plane (see Fig 3.1). At time  $t_1 > 0$ , the plate which is subjected to constant heat flux, starts moving impulsively in its own plane with uniform velocity,  $U$ . In our study, we consider the model equation (1.4) and use the expanded form of body force in equation (1.5) to get

$$\rho \left( \frac{\partial \mathbf{V}}{\partial t_1} + (\nabla \cdot \mathbf{V}) \mathbf{V} \right) = -\nabla P + \mu \nabla^2 \mathbf{V} + \rho(\mathbf{g} + \mathbf{J} \times \mathbf{B}) \quad (1.15)$$

Taking into account internal heat generation in fluid flow system, equation (1.6) can be written as

$$\rho C_p \left( \frac{\partial T}{\partial t_1} + (\mathbf{V} \cdot \nabla) T \right) = k \nabla^2 T + Q + \mu \phi + \frac{\mathbf{J}^2}{\sigma} \quad (1.16)$$

and according to [34, 36], equation of energy in terms of chemical species concentration due to the chemicals being constantly injected in the flow is given by

$$\left( \frac{\partial C_1}{\partial t_1} + (\mathbf{V} \cdot \nabla) C_1 \right) = D \nabla^2 C_1 \quad (1.17)$$

where  $k$ ,  $C_p$ ,  $Q$ ,  $D$  in equations (1.16) and (1.17) are respectively the thermal conductivity, specific heat capacity at constant pressure, internal heat generation, concentration diffusion coefficient.

Since the fluid is initially at rest, its velocity everywhere is zero, the fluid temperature is taken to be the free stream temperature,  $T_\infty$  and concentration is taken to be the free stream concentration,  $C_\infty$ . We therefore apply the following initial conditions.

For  $t_1 \leq 0$  :

$$u_1(y_1, 0) = 0, \quad w_1(y_1, 0) = 0 \quad (1.18)$$

and

$$T(y_1, 0) = T_\infty, \quad C_1(y_1, 0) = C_\infty \quad (1.19)$$

On the lower boundary, velocity component of the fluid along  $x_1$  direction assumes the plate velocity,  $U$  due to no slip effect, velocity along  $y_1$  axis is taken to be zero. Temperature on the lower boundary is due to heat diffusion caused by heat flux vector,  $q$  and concentration on the lower boundary is taken to be the wall (plate) concentration,  $C_{w_1}$ . Velocities  $u_1$  and  $w_1$  on the upper boundary are assumed to be zero. Hence

For  $t_1 > 0$  :

$$u_1(0, t_1) = U, \quad w_1(0, t_1) = 0, \quad \frac{\partial T}{\partial y_1} = -\frac{q}{k}, \quad C_1(0, t_1) = C_{w_1} \quad (1.20)$$

$$u_1(\infty, t_1) = 0, \quad w_1(\infty, t_1) = 0, \quad T(\infty, t_1) = T_\infty, \quad C_1(\infty, t_1) = C_\infty \quad (1.21)$$

We will then expand the body force term in equation (1.15) to include the Hall current and ion-slip term and further analysis of equations (1.16) and (1.17).

### **1.3 Objectives of the study**

The broad objective of this research was to formulate and solve governing MHD equations describing unsteady flow of a viscous, incompressible, electrically conducting fluid past an infinite porous flat plate subjected to mass transfer and convective heat exchange at the plate surface with the consideration of ion-slip and Hall current effect so as to evaluate and analyze the effects of thermo-physical parameters on the velocity profiles, temperature profiles and concentration profiles of the flow. The specific objectives of this study were:

1. To describe and analyze the effects of Hall currents, ion-slip on the velocity boundary layer thickness in the presence of cooling and heating of the plate by free convection currents.
2. To evaluate the effects of various thermo-physical parameters such as magnetic parameter, Grashof number, mass diffusion parameter, ion-slip parameter, Hall parameter, modified Grashof number, suction velocity on the solutal boundary layer, velocity and temperature profiles.
3. To evaluate and analyze how cooling of the plate by free convection currents affects the thermal boundary layer of an unsteady laminar fluid flow.

### **1.4 Significance of the study**

Magnetohydrodynamic mass and heat transfer is of considerable interest to mathematicians, scientists and engineers because it has many applications including design of MHD power generators and MHD pumps, MHD heat exchangers and design of ship propulsion

units. Our findings show that it can be possible to improve on the design of MHD pumps which operates on the principle that motion(force) on a fluid depends on magnitude of velocity of the fluid. The results also have the potential to serve as prototype for practical propulsion type of problems, for example, generation of propulsion force in moving ship

## **1.5 Research methodology**

For successful completion of this research, a good background knowledge of both numerical and analytical technique of solving differential equations is paramount. It is also a fact that equations governing MHD fluid flow are always non-linear and their exact solutions are difficult to obtain. A number of mathematicians researching on related areas for the case of steady MHD flows have used Newton-Raphson shooting method along with Runge-Kutta integration algorithms to numerically solve partial differential equations(p.d.e's) of momentum and energy balance governing MHD problems. Although Runge-Kutta is a powerful technique of solving differential equations numerically, it is used only in cases of steady p.d.e's and also it may not work satisfactorily in such cases where initial and boundary conditions are not "smooth" in nature as explained by Kumar [39]. Typical example is where the boundary condition changes abruptly from one time step to another as in our case with the velocity boundary condition since the plate is impulsively set in motion meaning velocity changes abruptly from its initial value of zero to  $U$  (plate velocity). We considered the general form of Navier-Stokes equation of momentum, incorporated the hall and ion-slip current terms in the body force factor and formed the velocity equations. The equation of energy in terms of temperature was formed where the contribution of constant heat flux arising from convective heat transfer and concentration diffusion gradient were taken into consideration to give the total heat energy of the system. In forming the p.d.e, we considered the fact that the fluid flow is along  $x_1$  axis and the presence of suction velocity at the plate. Since the formulated coupled partial differential equations in the present study were non-linear and because the flow is unsteady, only finite difference method can be used to solve the p.d.e. We used

an explicit scheme of finite difference technique in solving the unsteady partial differential equations of the continuity, momentum and energy balance governing the problem. We first studied in details the specific p.d.e, carried out transformations using complex transform, injected the initial and boundary conditions imposed on the problem, carried out stability analysis to check and ascertain that the finite difference scheme used in finding solutions in this study is both convergent and stable. We then developed a mathematica code, executed the simplified explicit difference equations, presented the results graphically. We discussed and analyzed the results for the effects Hall and ion-slip currents on the velocity profiles due to both cooling and heating of the plate by free convectioal currents. We also evaluated the effects of various thermo-physical parameters on concentration, temperature and velocity profiles of the flow. Conclusions were drawn from the findings and then finally we put forward recommendations.

## CHAPTER 2

### LITERATURE REVIEW

#### 2.1 MHD flows past infinite plates

In 1956, Shercliff [24] studied the steady motion of an electrically conducting fluid in pipes under transverse magnetic fields. He investigated the ultimate steady velocity profile and its associated pressure gradient. His results showed that pressure drop associated with the adjustment of the velocity profile is found to be independent of field strength. His work did not take into account the induced electric potential. Gebhart and Mollendorf [7] in 1969 studied viscous dissipation in external natural convective flows and found out that viscous dissipative heat is important when the free convective flow field is of extreme size or the flow is at extremely low temperature. This has become the basis of considering viscous fluid flows subjected to constant heat flux. Their work failed to show how viscous forces contribute to the overall velocity profiles. In 1978, Ram and Singh [23] studied steady laminar flow of an electrically conducting fluid through a channel in the presence of a transverse magnetic field under the influence of a periodic pressure gradient and solved the resulting differential equations by the method of Laplace transform. Their findings which showed variation of velocities with pressure gradient parameter were only based on weak magnetic field i.e  $M = 1.0$ ,  $M = 1.5$  and  $M = 2.0$  and no consideration of ion-slip effects. Soundalgekar et al [12] in 1979 investigated the problem of free convection effects on Stokes problem for a vertical plate with transverse applied magnetic field. In the year 1986, Sahoo et al [32] investigated the unsteady free convection and mass transfer effect on the flow past a uniformly accelerated infinite non-conducting vertical plate through a porous medium in the presence of a uniform magnetic field and showed that temperature increases with increase in variable thermal conductivity and decreases with increasing radiation and suction velocity. In their research, Hall current and ion-slip current were ignored. It was established by Naidu et al in 1987 when they studied boundary layer heat transfer with electromagnetic fields that the velocity boundary layer is reduced

by the effects of transverse magnetic field for some compressible MHD fluids while the temperature profiles are increased. Naidu's findings were only limited to cases of varying pressure gradient with no consideration of mass transfer and suction at the boundary. Dikshit et al [13] in 1988 studied hydrodynamic flow past a continuously moving semi-infinite plate with large suction and assumed the effects hall current while using relatively weak magnetic field but the current trend in MHD studies is to use a strong magnetic fields. A gain in the year, 1988, Singh and Sacheti [40] reported the results of their study of hydromagnetic free convection flow with constant heat flux where it was observed that the magnetic parameter had a retarding effect on the flow velocity. However, nothing was mentioned with regard to the contribution of either Hall current or ion-slip current to the velocity profiles of the flow. Special cases of this topic have also been studied by Mansour et al [26] in 1990 in connection with emerging questions. When the scholars investigated the influence of lateral mass flux on free convection flow past a vertical flat plate embedded in a saturated porous medium and with the aim of providing solutions to the effects of electromagnetic fields on the boundary layer flow. They analyzed the effects magnetic parameter, Grashoff number, suction velocity on velocity, temperature flow fields. However, the general information available in the application of strong magnetic fields, effects of ion slip currents was still remarkably scarce. Convective heat and mass transfer of a viscous flow past a hot vertical plane wall with periodic heat sources was studied by Dash and Tripathy [31] in 1993. Although their findings for velocity profiles as affected by weak magnetic fields were in line by the previous findings, there arose the need to apply strong magnetic fields. Ram et al [27] in the year 1995 solved the MHD Stokes problem of convective flow from a vertical infinite plate in a rotating fluid and found out that an increase in hall parameter leads to an increase in primary velocity profiles for large Grashof numbers. There was no mention of ion-slip effects. Elbashbeshy [10] in 1997 studied MHD heat and mass transfer problem a long a vertical plate under the combined buoyancy effects of thermal and species diffusion and established that in fluid flow where the buoyancy forces are strong (larger Grashof number), then buoyancy forces drives natural convection while viscous force retards fluid velocity but he did not factor

in the effects of hall currents. Yih [9] in 1999 studied the free convection effect on MHD coupled heat and mass transfer of a moving permeable vertical surface. The analysis of steady flow resulted in findings of effects of thermo-physical parameters on the fluid flow patterns but failed to take into account the effects of ion-slip current since the study was for a steady flow. In 2001, Soundalgekar et al [12] investigated the problem of free convection effects on Stokes problem for a vertical plate with transverse applied magnetic field. Their findings were based on smaller values of magnetic parameter ( $M < 5.0$ ).

## **2.2 MHD free convection flows**

Seddeek [20] in 2001 studied the thermal radiation and buoyancy effects on MHD free convection heat generation flow over an accelerating permeable surface with temperature dependent viscosity and concentrated more on analyzing the effects of buoyancy forces on fluid velocity. Also Kinyanjui et al [30] in 2001 presented their work on MHD free convection heat and mass transfer of a heat generating fluid past an impulsively started infinite vertical porous plate with hall current and heat absorption. An analysis of the effects of the parameter of skin friction, rates of mass and heat transfer on velocity was reported with no analysis to combined effects of Hall and ion-slip on flow fields but only examining isolated effects of hall parameter on the fluid flow fields. Azzam [6] in 2002, carried out a study on the radiation effects on the MHD mixed free-forced convection flow past a semi-infinite moving vertical plate for high temperature differences and reported the effects of radiation parameters along with Eckert and magnetic numbers how they cause variation on velocity and temperature profiles of a fluid flow. There was no attempt to impose suction on the plate and also include ion-slip effect on the fluid flow. In the same year, Takha et al [8] investigated electrically conducting fluid in an unsteady magnetohydrodynamics fluid flow for heat transfer in an ambient fluid and came up with results that showed thick velocity boundary flow for increasing modified Grashof number. But still their was consideration of lower values of magnetic fields. In the year, 2004 Ghally and Seddeek [14] investigated the effects of chemical reactions, heat and mass

transfer on laminar flow along a semi-infinite horizontal plate with temperature dependent viscosity and showed that for cooling of the plate by free convection, velocity profiles of the flow increases with increase in modified Grashof number,  $G_c$ . No investigations were made concerning a case of heating the plate by free convection currents. Unsteady MHD convective heat transfer past a semi-infinite vertical permeable moving plate with heat absorption was also reported by Chamka [4] in the same year and the analysis was more on thermo-physical parameters excluding ion-slip currents and he showed that to some extent, fluid velocity is retarded by the presence of increasing values of magnetic parameter in the flow. In 2005, Chandra [34] investigated steady MHD flow of an electrically conducting fluid between two parallel infinite plate when the upper plate is made to move with constant velocity while the lower plate is stationary. His findings were on the effects magnetic parameter, Eckert number and magnetic Reynold number on velocity and temperature profiles. However, there was no mention of Hall and ion-slip currents because the study was mainly on steady flow and time is a factor current. Cortell [21] in 2007 analyzed MHD mass transfer for two classes of viscoelastic fluid over a porous stretching sheet. The influence of magnetic parameter, Viscoelastic parameter on the boundary layer were reported, he concluded that for a given viscoelastic fluid subjected to a constant suction, the work done due to deformation effect increases with increase in the magnetic parameter,  $M$ . Although Cortell considered a case of a viscoelastic fluid, he did not mention anything on ion-slip current. Again in 2007 Ganesh and Krishnambal [25] studied unsteady MHD Stokes flow of a viscous fluid between two parallel porous plate. They considered fluid being withdrawn through both walls of the channel at the same rate. They obtained exact solution for all values of Suction Reynolds number,  $R$  and magnetic parameter,  $M$ . It was found out that in the presence of a transverse magnetic field the fluid is being withdrawn through both walls of the channel at the rate. There was no consideration of effects ion-slip or Hall currents of flow velocity. Bataller [16] in 2008 explored Sakiadis and Blasius flow problems with convective boundary effects and considering a case of constant wall temperature where he investigated fluid-solid interface characteristics for different values of Prandtle,  $P_r$  and radiation parameter,  $N_r$ . His

results reflected a numerical solution for a combined effects of thermal radiation and convective surface heat flow. He did not tackle cases of cooling of the plate by free convection with constant heat flux. He also neglected ion-slip currents. In the same year, 2008, the effects of thermal radiation on heat and mass transfer flow of a variable viscosity fluid past a vertical porous plate permeated by a transverse magnetic field was reported by Makinde et al [15]. They discovered that flow patterns of the fluid are greatly affected by heating of the plate by free convection. However, there was no mention in their work, the combined effects of Hall current and ion-slip parameter.

Makinde [17] again in 2009 considered a steady MHD flow past a semi-infinite porous plate with constant heat flux. In his work, Hall current effects were neglected. He solved the Pde equations governing the flow by Newton-Raphson shooting method along with fourth order Runge-kutta integration algorithm. His findings revealed that for positive values of the buoyancy parameter, the skin friction increases with increase in  $E_c$  and decreases with increasing values of permeability parameter. In his work, Hall current effects were neglected. Within the same year, Rajeswari et al [19] investigated the effect of chemical reaction, heat and mass transfer on non-linear MHD boundary layer flow through a stationary vertical porous surface in the presence of suction with power law surface temperature and concentration. Their findings showed that velocity boundary thickness increases with increase Grashof number, time but decreases with increase in Hartman number. Still in their study, effects of ion-slip currents were neglected in their study. Also in 2009, Beg et al [33] in their work investigated numerically the free convection MHD heat and mass transfer from a stretching surface to a saturated porous medium with Soret and Dufour effects. They used a small magnetic parameter(  $M = 0.1$ ) signifying a very weak magnetic field and negligible internal heat source. Towards the end of 2009, Aziz [3] researched on steady MHD thermal boundary layer flow and demonstrated that a similarity solution is only possible if the convective heat transfer associated with the hot fluid on the lower surface of the plate is proportional to  $x^{-\frac{1}{2}}$ . His results showed that for a constant heat flux, Representative Prandtl numbers of 0.1 - 0.72 or 7.0 - 10.0 for computations can be carried out for air or water respectively. Where as Aziz's findings have become applicable in many computational modeling involving hydromagnetic fluids, his work fell short of including the isolated or complementary effects of Hall and ion-slip currents in an MHD fluid flow. Sacheti and Singh [32] in 2010 studied MHD free-convective flow with constant heat flux and reported an oscillatory behavior of the velocity profiles with changing magnetic parameter and attributed his results

to a low value of external applied magnetic field and because of excess cooling of the plate. This means that the current trend is towards using a stronger magnetic field and moderate cooling of the plate.

In view of the findings of mathematicians' work in the field of computational modeling of MHD liquid flows, no study appeared to have considered the combined effects of ion-slip current, Hall current and convective mass transfer over an infinite plate surface for a boundary layer flow, which is the focus of our research. We therefore considered hydromagnetic mass and heat transfer over a flat surface as was investigated by Aziz [3], modified his work to the case of unsteady flow and included the combined effect of ion-slip current, Hall current and the convective heat exchange at the plate on the boundary layer flow.

## CHAPTER 3

### MATHEMATICAL FORMULATION

#### 3.1 Problem setting

We consider a flat horizontal porous plate which is impulsively set into motion with a uniform velocity  $U$  along the  $x_1$ -axis at the time,  $t_1 > 0$  (see Figure 3.1). But initially, at the time,  $t_1 = 0$ , the plate is at rest. A uniform magnetic field,  $B_0$  is applied perpendicular to the plate. The fluid velocity components are  $(u_1, v_1, w_1)$  relative to the frame of reference.

There is uniform injection of chemical species whose concentration is limited to the fluid density. The temperature and concentration of the fluid over the plate is taken to be  $T_\infty$  and  $C_\infty$  respectively. The lower surface of the plate is heated by convection from a hot fluid at a temperature,  $T_f$ . The plate is porous and there is constant sipping out of some fluid a cross the plate at a constant velocity of  $v_0^*$ . Since the plate is infinite in extent and the flow is unsteady, the physical variables such as velocity, temperature and concentration are functions of  $y_1$  and  $t_1$  only.

Given that density of the fluid,  $\rho$  is constant, the equation of continuity given in equation (1.3) is expressed as

$$\frac{\partial u_1}{\partial x_1} + \frac{\partial v_1}{\partial y_1} + \frac{\partial w_1}{\partial z_1} = 0 \quad (3.1)$$

Considering the suction velocity at the plate,  $v_0^*$ , then the velocity component along the  $y_1$ -axis,  $v_1$ , everywhere in the flow is given by

$$v_1 = -v_0^* \quad (3.2)$$

using equation (3.2) and the fact that velocity components depend on  $y$  and  $t$  only, equation (3.1) becomes zero on both sides. This shows that mass is conserved.

The Navier-Stokes momentum equation given in equation (1.4) can be expressed as

$$\frac{\partial \mathbf{V}}{\partial t_1} + (\nabla \cdot \mathbf{V})\mathbf{V} = -\frac{1}{\rho}\nabla P + \frac{\mu}{\rho}\nabla^2 \mathbf{V} + \mathbf{f}_B \quad (3.3)$$

where  $\mathbf{f}_B$  is the sum total of all the body forces and the other symbols are as defined in the index of notations. Since all variables depend on  $y_1$  and  $t_1$  only,

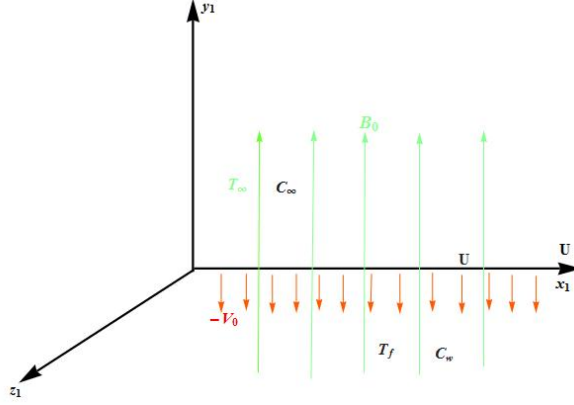


Figure 3.1: Flow configuration with the coordinate system

equation (3.3) in components form gives

$$\frac{\partial u_1}{\partial t_1} - v_0^* \frac{\partial u_1}{\partial y_1} = -\frac{1}{\rho} \frac{\partial P}{\partial y_1} + \frac{\mu}{\rho} \frac{\partial^2 u_1}{\partial y_1^2} + (f_B)_{x_1} \quad (3.4)$$

$$\frac{\partial v_0^*}{\partial t_1} + v_0^* \frac{\partial v_0^*}{\partial y_1} = -\frac{1}{\rho} \frac{\partial P}{\partial y_1} - \frac{\mu}{\rho} \frac{\partial^2 v_0^*}{\partial y_1^2} + (f_B)_{y_1} \quad (3.5)$$

$$\frac{\partial w_1}{\partial t_1} - v_0^* \frac{\partial w_1}{\partial y_1} = -\frac{1}{\rho} \frac{\partial P}{\partial y_1} + \frac{\mu}{\rho} \frac{\partial^2 w_1}{\partial y_1^2} + (f_B)_{z_1} \quad (3.6)$$

where  $(f_B)_{x_1}$  in equation (3.4),  $(f_B)_{y_1}$  in equation (3.5) and  $(f_B)_{z_1}$  in equation (3.6) are components of body force vector,  $\mathbf{f}_B$  along  $x_1$ ,  $y_1$  and  $z_1$  directions respectively. Suction velocity,  $v_0^*$  is assumed to be constant everywhere in the flow, hence, equation (3.5) reduces to

$$0 = -\frac{1}{\rho} \frac{\partial P}{\partial y_1} + (f_B)_{y_1} \quad (3.7)$$

## 3.2 Mathematical analysis

The component of the body force along  $y_1$ -axis is negligible given that the motion of the fluid is along  $x_1$  direction and is mainly caused by forces in the same direction, meaning  $(f_B)_{y_1} \approx 0$ , equation (3.7) shows the constancy of pressure along  $y_1$ -axis and everywhere in the flow since pressure gradient along  $x_1$  and  $y_1$  is zero. Under the usual Boussinesq and Oberbeck approximations as explained by Aziz [3], considering that heat transfer can reasonably cause significant changes in the transport proportions in an incompressible viscous fluid flow, the contribution of temperature difference and concentration difference to body force term are respectively given by  $g\beta_T(T - T_\infty)$  and  $g\beta_c(C_1 - C_\infty)$  and they also have the effect of causing movement of fluid particle along  $x_1$  direction. The Lorentz force, along  $x_1$  and  $z_1$  directions are respectively given by  $B_{y_1}J_{z_1}$  and  $B_{y_1}J_{x_1}$  with their directions determined by Fleming's clock rule. Therefore equations (3.4) and (3.6) which are respectively equations of motion along  $x_1$  and  $z_1$  directions become

$$\frac{\partial u_1}{\partial t_1} - v_0^* \frac{\partial u_1}{\partial y_1} = g\beta_T(T - T_\infty) + g\beta_c(C_1 - C_\infty) + \frac{\mu}{\rho} \frac{\partial^2 u_1}{\partial y_1^2} + \frac{B_{y_1}}{\rho} J_{z_1} \quad (3.8)$$

$$\frac{\partial w_1}{\partial t_1} - v_0^* \frac{\partial w_1}{\partial y_1} = \frac{\mu}{\rho} \frac{\partial^2 w_1}{\partial y_1^2} - \frac{B_{y_1}}{\rho} J_{x_1} \quad (3.9)$$

where  $g$ ,  $\beta_T$ ,  $T$ ,  $T_\infty$ ,  $\beta_c$ ,  $C_1$ ,  $C_\infty$ ,  $\mu$ ,  $B_{y_1}$ ,  $J_{z_1}$ ,  $J_{x_1}$  and  $\rho$  in equations (3.8) and (3.9) are respectively the gravitational field strength, thermal expansion coefficient, dimensional temperature, dimensional free stream temperature, concentration expansion coefficient, dimensional concentration of the injected material, dimensional free stream concentration, dynamic viscosity coefficient, magnetic field vector in  $y_1$ -direction, current density in  $z_1$  direction, current density in  $x_1$  direction and fluid density.

The fluid is electrically conducting with minimal electrical resistance implying that electric current due to Hall and ion slip effects produces insignificant heat energy (joule heating) in the system. Given that the contribution of joule heating to the total heat energy is very minimal, then equation (1.16) which is the equation of energy for the temperature can be written as

$$\rho C_p \left( \frac{\partial T}{\partial t} + (\mathbf{V} \cdot \nabla) T \right) = k \nabla^2 T + \mu \phi + Q \quad (3.10)$$

where  $k$ ,  $\phi$  and  $Q$  are thermal conductivity, thermal energy due to dissipative heat and internal heat generation respectively. Thermal energy due to dissipative heat,

$\phi$  along  $y_1$  direction is given by

$$\phi = \left(\frac{\partial u_1}{\partial y_1}\right)^2 + \left(\frac{\partial v_0^*}{\partial y_1}\right)^2 + \left(\frac{\partial w_1}{\partial y_1}\right)^2 \quad (3.11)$$

Considering that temperature is dependent on  $y_1$  and  $t_1$  only, the components of equation (3.10) along  $x_1$  and  $z_1$  reduces to zero. Using equation (3.11) in equation (3.10) and on simplification, the  $y_1$  component of equation (3.10) is given as

$$\frac{\partial T}{\partial t_1} - v_0^* \frac{\partial T}{\partial y_1} = \frac{k}{\rho C_p} \frac{\partial^2 T}{\partial y_1^2} + \frac{\mu}{\rho C_p} \left( \left(\frac{\partial u_1}{\partial y_1}\right)^2 + \left(\frac{\partial w_1}{\partial y_1}\right)^2 \right) + \frac{Q}{\rho C_p} \quad (3.12)$$

The species concentration can be given in form of the convective-diffusion equation as

$$\frac{\partial C_1}{\partial t_1} - v_0^* \frac{\partial C_1}{\partial y_1} = D \frac{\partial^2 C_1}{\partial y_1^2} \quad (3.13)$$

where  $D$  is the concentration diffusion coefficient. Equations (3.8), (3.9), (3.12), and (3.13) are the main equations for considerations where  $J_{z_1}$  and  $J_{x_1}$  in equations (3.8) and (3.9) are to be analyzed. Since heat is uniformly applied to the plate, we apply Fourier's law of heat conduction as given by Manyonge [36] as

$$\frac{\partial T}{\partial y_1} = -\frac{q}{k} \quad (3.14)$$

For simplicity, internal heat generation in the system as explained by Chandra [34] is assumed to be given as  $\frac{qv}{kU}Q$ , where  $U$  is the velocity of the plate.

From the setting of the problem as indicated in the statement of the problem, we apply the following initial and boundary conditions

For  $t_1 \leq 0$  :

$$u_1(y_1, 0) = 0, \quad w_1(y_1, 0) = 0 \quad (3.15)$$

and

$$T(y_1, 0) = T_\infty, \quad C_1(y_1, 0) = C_\infty \quad (3.16)$$

For  $t_1 > 0$  :

$$u_1(0, t_1) = U, \quad w_1(0, t_1) = 0, \quad \frac{\partial T}{\partial y_1} = -\frac{q}{k}, \quad C_1(0, t_1) = C_w \quad (3.17)$$

and

$$u_1(\infty, t_1) = 0, \quad w_1(\infty, t_1) = 0, \quad T(\infty, t_1) = T_\infty, \quad C_1(\infty, t_1) = C_\infty \quad (3.18)$$

Considering the effects of ion-slip currents as given by Chandra [34], the generalized Ohm's law is given as

$$\mathbf{J} = \sigma(\mathbf{E} + \mathbf{V} \times \mathbf{B}) - \frac{\omega_e \tau_e}{B_0} (\mathbf{J} \times \mathbf{B}) - \frac{\omega_e \tau_e \beta_n}{B_0^2} ((\mathbf{J} \times \mathbf{B}) \times \mathbf{B}) \quad (3.19)$$

where  $\mathbf{B}$ ,  $\mathbf{E}$ ,  $\mathbf{V}$ ,  $\mathbf{J}$ ,  $\sigma$ ,  $\omega_e$ ,  $\tau_e$ ,  $\beta_n$  are respectively the magnetic field vector, the electric field vector ( $\mathbf{E} = [E_{x_1}, E_{y_1}, E_{z_1}]$ ), the fluid velocity vector ( $\mathbf{V} = [u_1, v_1, w_1]$ ), the current density vector, the heat conductivity of the fluid, the cyclotron frequency, the electron collision time and the ion-slip parameter.

For partially ionized fluids, the magnetic Reynolds number may be neglected since the induced magnetic field is negligible in comparison to the applied magnetic field but the effects of viscous dissipation in the fluid is taken into account as indicated by Kinyanjui et al [30]. Given that  $\mathbf{B} \equiv (B_{x_1}, B_{y_1}, B_{z_1})$  and in the absence of free magnetic poles, the solenoidal relation,  $\nabla \cdot \mathbf{B} = 0$  implies that  $B_{y_1} = B_0 = \text{constant}$  everywhere in the flow. The equation of the conservation of electric charge  $\nabla \cdot \mathbf{J} = 0$  where  $\mathbf{J} \equiv (J_{x_1}, J_{y_1}, J_{z_1})$  gives  $J_{y_1} = \text{constant}$ . This constant is zero since  $J_{y_1} = 0$  at each point on the plate which is electrically non-conducting. Thus  $J_{y_1} = 0$  everywhere in the flow. From the assumption that the induced magnetic fields are neglected, then the Maxwell's equation (Faraday's law of induction) given in equation (1.7) becomes

$$\nabla \times \mathbf{E} = 0 \quad (3.20)$$

which gives

$$\frac{\partial E_{x_1}}{\partial x_1} = 0 \quad (3.21)$$

and

$$\frac{\partial E_{z_1}}{\partial z_1} = 0 \quad (3.22)$$

Equations (3.21) and (3.22) implies that  $E_{x_1}$  and  $E_{z_1}$  which are electric field vectors along  $x_1$ -axis and  $z_1$ -directions respectively are constant everywhere in the flow.

Equation (3.19) can therefore be expressed into components form along the  $x_1$  and  $z_1$  directions only since  $J_{y_1} = 0$ . Therefore equating the  $x_1$  and  $z_1$  components of equation (3.19) we get

$$J_{x_1} = \sigma(-E_{x_1} + w_1 B_y) - \frac{\omega_e \tau_e B_{y_1} J_{z_1}}{B_0} - \frac{\omega_e \tau_e \beta_n J_{x_1}}{B_0^2} \quad (3.23)$$

and

$$J_{z_1} = \sigma(-E_{z_1} + u_1 B_y) + \frac{\omega_e \tau_e B_{y_1} J_{x_1}}{B_0} - \frac{\omega_e \tau_e \beta_n J_{z_1}}{B_0^2} \quad (3.24)$$

In view of the above assumptions made on magnitude of magnetic field vector,  $\mathbf{B}$ , and that  $B_0^2 \equiv B_0 \cdot B_0 = 1$  as explained by Makinde [17], equations (3.23) and (3.24) are simplified to give us

$$J_{x_1} = \sigma(-E_{x_1} + w_1 B_0) - \omega_e \tau_e J_{z_1} - \omega_e \tau_e \beta_n J_{x_1} \quad (3.25)$$

and

$$J_{z_1} = \sigma(-E_{z_1} + u_1 B_0) + \omega_e \tau_e J_{x_1} - \omega_e \tau_e \beta_n J_{z_1} \quad (3.26)$$

Choosing  $\beta_m = \omega_e \tau_e$  as the Hall current parameter and rearranging equations (3.25) and (3.26) we get

$$J_{x_1}(1 + \beta_m \beta_n) - \beta_m J_{z_1} = \sigma E_{x_1} - \sigma B_0 w_1 \quad (3.27)$$

and

$$J_{z_1}(1 + \beta_m \beta_n) + \beta_m J_{x_1} = \sigma E_{z_1} + \sigma B_0 u_1 \quad (3.28)$$

To get the current densities  $J_{x_1}$  and  $J_{z_1}$ , we solve equations (3.27) and (3.28) simultaneously giving

$$J_{x_1} = \frac{\sigma[(1 + \beta_m \beta_n)(E_{x_1} - B_0 w_1) + \beta_m(E_{z_1} + B_0 u_1)]}{(1 + \beta_m \beta_n)^2 + \beta_m^2} \quad (3.29)$$

$$J_{z_1} = \frac{\sigma[(1 + \beta_m \beta_n)(E_{z_1} + B_0 u_1) - \beta_m(E_{x_1} - B_0 w_1)]}{(1 + \beta_m \beta_n)^2 + \beta_m^2} \quad (3.30)$$

Using equations (3.29) and (3.30), the equations of motion along  $x_1$  and  $z_1$  directions as shown in equations (3.8) and (3.9) become

$$\begin{aligned} \frac{\partial u_1}{\partial t_1} - v_0^* \frac{\partial u_1}{\partial y_1} &= g\beta_T(T - T_\infty) + g\beta_c(C_1 - C_\infty) + \frac{\mu}{\rho} \frac{\partial^2 u_1}{\partial y_1^2} - \\ &\frac{\sigma B_0[(1 + \beta_m \beta_n)(E_{z_1} + B_0 u_1) - \beta_m(E_{x_1} - B_0 w_1)]}{\rho[(1 + \beta_m \beta_n)^2 + \beta_m^2]} \end{aligned} \quad (3.31)$$

$$\frac{\partial w_1}{\partial t} - v_0^* \frac{\partial w_1}{\partial y_1} = \frac{\mu}{\rho} \frac{\partial^2 w_1}{\partial y_1^2} - \frac{\sigma B_0[(1 + \beta_m \beta_n)(E_{x_1} - B_0 w_1) + \beta_n(E_{z_1} + B_0 u_1)]}{\rho[(1 + \beta_m \beta_n)^2 + \beta_n^2]} \quad (3.32)$$

The electric field vector  $E_{z_1}$  along the  $z_1$ - axis produces force equivalent to  $-B_0U$  according to the usual Fleming's law of electromagnetic induction as explained by Chandra [34], where  $U$  is the plate velocity. The effect of electric field vector  $E_{x_1}$  on the flow is infinitesimal and so  $E_{x_1} \approx 0$ . Equations (3.31) and (3.32) are therefore reduced to equations (3.33) and (3.34) respectively.

$$\frac{\partial u_1}{\partial t_1} - v_0^* \frac{\partial u_1}{\partial y_1} = g\beta_T(T - T_\infty) + g\beta_c(C_1 - C_\infty) + \nu \frac{\partial^2 u_1}{\partial y_1^2} - \frac{\sigma B_0^2 [(1 + \beta_m \beta_n)(u_1 - U) + \beta_m w_1]}{\rho[(1 + \beta_m \beta_n)^2 + \beta_m^2]} \quad (3.33)$$

$$\frac{\partial w_1}{\partial t_1} - v_0^* \frac{\partial w_1}{\partial y_1} = \nu \frac{\partial^2 w_1}{\partial y_1^2} - \frac{\sigma B_0^2 \{(1 + \beta_m \beta_n)w_1 - \beta_m(u_1 - U)\}}{\rho[(1 + \beta_m \beta_n)^2 + \beta_m^2]} \quad (3.34)$$

The dimensional equations (3.33) and (3.34) together with (3.12) and (3.13) which are the model equations to be solved are converted to non-dimensional form. We define the dimensionless quantities as follows:

Let

$$u = \frac{u_1}{U}, w = \frac{w_1}{U}, v_0 = \frac{v_0^*}{U}$$

$$y = \frac{y_1 U}{\nu}, t = \frac{t_1 U^2}{\nu}, C = \frac{C_1 - C_\infty}{C_w - C_\infty}$$

$$\theta = \frac{T - T_\infty}{\left(\frac{q\nu}{kU}\right)}$$

Equations (3.12), (3.13), (3.33) and (3.34) are dimensionalized giving us

$$\frac{U^3}{\nu} \frac{\partial u}{\partial t} - \frac{v_0 U^3}{\nu} \frac{\partial u}{\partial y} = g\beta_T \theta \left(\frac{q\nu}{kU}\right) + g\beta_c (C_w - C_\infty) C + \frac{U^3}{\nu} \frac{\partial^2 u}{\partial y^2} - \frac{\sigma B_0^2 [(1 + \beta_m \beta_n)(uU - U) + \beta_m wU]}{\rho[(1 + \beta_m \beta_n)^2 + \beta_m^2]} \quad (3.35)$$

$$\frac{U^3}{\nu} \frac{\partial w}{\partial t} - \frac{v_0 U^3}{\nu} \frac{\partial w}{\partial y} = \frac{U^3}{\nu} \frac{\partial^2 w}{\partial y^2} - \frac{\sigma B_0^2 [(1 + \beta_m \beta_n)wU - \beta_m(uU - U)]}{\rho[(1 + \beta_m \beta_n)^2 + \beta_m^2]} \quad (3.36)$$

$$\begin{aligned} \frac{U^2}{\nu} \left( \frac{q\nu}{kU} \right) \frac{\partial \theta}{\partial t} - \frac{v_0 U^2}{\nu} \left( \frac{q\nu}{kU} \right) \frac{\partial \theta}{\partial y} &= \frac{U^2 k}{\rho C_p \nu^2 \left( \frac{q\nu}{kU} \right)} \frac{\partial^2 \theta}{\partial y^2} + \frac{Q\nu}{\rho C_p U^2 \left( \frac{q\nu}{kU} \right)} + \\ &\frac{U^4}{\nu^2 C_p} \left[ \left( \frac{\partial u}{\partial y} \right)^2 + \left( \frac{\partial w}{\partial y} \right)^2 \right] \end{aligned} \quad (3.37)$$

$$(C_w - C_\infty) \frac{U^2}{\nu} \frac{\partial C}{\partial t} - (C_w - C_\infty) \frac{v_0 U^2}{\nu} \frac{\partial C}{\partial y} = (C_w - C_\infty) D \frac{U^2}{\nu^2} \frac{\partial^2 C}{\partial y^2} \quad (3.38)$$

On dividing equations (3.35) and (3.36) all through by  $\frac{U^3}{\nu}$ , equation (3.37) all through by  $\frac{U^2}{\nu} \left( \frac{q\nu}{kU} \right)$  and equation (3.38) all through by  $(C_w - C_\infty) \frac{U^2}{\nu}$ , we have

$$\begin{aligned} \frac{\partial u}{\partial t} - v_0 \frac{\partial u}{\partial y} &= \frac{\nu g \theta \beta_T \left( \frac{q\nu}{kU} \right)}{U^3} + \frac{\nu g \beta_c (C_w - C_\infty) C}{U^3} + \frac{\partial^2 u}{\partial y^2} - \\ &\frac{\nu \sigma B_0^2 [(1 + \beta_m \beta_n)(u - 1) + \beta_m w]}{U^2 \rho [(1 + \beta_m \beta_n)^2 + \beta_m^2]} \end{aligned} \quad (3.39)$$

$$\frac{\partial w}{\partial t} - v_0 \frac{\partial w}{\partial y} = \frac{\partial^2 w}{\partial y^2} - \frac{\nu \sigma B_0^2 [(1 + \beta_m \beta_n)w - \beta_m (u - 1)]}{U^2 \rho [(1 + \beta_m \beta_n)^2 + \beta_m^2]} \quad (3.40)$$

$$\frac{\partial \theta}{\partial t} - v_0 \frac{\partial \theta}{\partial y} = \frac{k}{\rho \nu C_p} \frac{\partial^2 \theta}{\partial y^2} + \frac{Q\nu}{\rho C_p U^2 \left( \frac{q\nu}{kU} \right)} + \frac{U}{C_p \left( \frac{q\nu}{kU} \right)} \left[ \left( \frac{\partial u}{\partial y} \right)^2 + \left( \frac{\partial w}{\partial y} \right)^2 \right] \quad (3.41)$$

$$\frac{\partial C}{\partial t} - v_0 \frac{\partial C}{\partial y} = \frac{D}{\nu} \frac{\partial^2 C}{\partial y^2} \quad (3.42)$$

Equations (3.39) to (3.42) can be written as

$$\frac{\partial u}{\partial t} - v_0 \frac{\partial u}{\partial y} = G_r \theta + G_c C + \frac{\partial^2 u}{\partial y^2} - \frac{M^2 [(1 + \beta_m \beta_n)(u - 1) + \beta_m w]}{[(1 + \beta_m \beta_n)^2 + \beta_m^2]} \quad (3.43)$$

$$\frac{\partial w}{\partial t} - v_0 \frac{\partial w}{\partial y} = \frac{\partial^2 w}{\partial y^2} - \frac{M^2 [(1 + \beta_m \beta_n)w - \beta_m (u - 1)]}{[(1 + \beta_m \beta_n)^2 + \beta_m^2]} \quad (3.44)$$

$$\frac{\partial \theta}{\partial t} - v_0 \frac{\partial \theta}{\partial y} = \frac{1}{P_r} \frac{\partial^2 \theta}{\partial y^2} - \frac{B_i \theta}{P_r} + E_c \left[ \left( \frac{\partial u}{\partial y} \right)^2 + \left( \frac{\partial w}{\partial y} \right)^2 \right] \quad (3.45)$$

$$\frac{\partial C}{\partial t} - v_0 \frac{\partial C}{\partial y} = S_c \frac{\partial^2 C}{\partial y^2} \quad (3.46)$$

where

$G_r = \frac{\nu g \theta \beta_T}{U^3} \left( \frac{q\nu}{kU} \right)$  is the Grashof number,

$G_c = \frac{\nu g \beta_c (C_w - C_\infty)}{U^3}$  is the modified Grashof number,

$M = \left[ \left( \frac{\sigma\nu}{\rho} \right)^{\frac{1}{2}} \frac{B_0}{U} \right]$  is the Hartmann number,

$P_r = \frac{\nu \rho C_p}{k} = \frac{\mu c_p}{k}$  is the Prandtl number,

$B_i = \frac{Q\nu}{kU^2}$  is the convective heat exchange parameter,

$E_c = \frac{U}{C_p \left( \frac{q\nu}{kU} \right)}$  is the Eckert number,

$S_c = \frac{D}{\nu}$  is the mass diffusion parameter.

The initial and boundary conditions are non-dimensionalized so as to get

For  $t \leq 0$  :

$$u(y, 0) = 0, \quad w(y, 0) = 0 \quad (3.47)$$

and

$$\theta(y, 0) = 0, \quad C(y, 0) = 0 \quad (3.48)$$

For  $t > 0$  :

$$u(0, t) = 1, \quad w(0, t) = 0, \quad \theta(0, t) = 1, \quad C(0, t) = 1 \quad (3.49)$$

and

$$u(\infty, t) = 0, \quad w(\infty, t) = 0, \quad \theta(\infty, t) = 0, \quad C(\infty, t) = 0 \quad (3.50)$$

In order to reduce the number of equations at the present level, we apply complex transformation as follows:  $Z = u + iw - 1$ , where  $i = \sqrt{-1}$  and  $\bar{Z} = u - iw - 1$  the complex conjugate of  $Z$ . So that

$$\frac{\partial Z}{\partial t} = \frac{\partial u}{\partial t} + i \frac{\partial w}{\partial t},$$

$$\frac{\partial Z}{\partial y} = \frac{\partial u}{\partial y} + i \frac{\partial w}{\partial y},$$

$$\frac{\partial^2 Z}{\partial y^2} = \frac{\partial^2 u}{\partial y^2} + i \frac{\partial^2 w}{\partial y^2}$$

and

$$\begin{aligned} \frac{\partial Z}{\partial y} \cdot \frac{\partial \bar{Z}}{\partial y} &= \left( \frac{\partial u}{\partial y} + i \frac{\partial w}{\partial y} \right) \cdot \left( \frac{\partial u}{\partial y} - i \frac{\partial w}{\partial y} \right) \\ &= \left( \frac{\partial u}{\partial y} \right)^2 + \left( \frac{\partial w}{\partial y} \right)^2 \end{aligned}$$

Adding equations (3.43) and (3.44) together, we get

$$\begin{aligned} \frac{\partial u}{\partial t} + \frac{\partial w}{\partial t} - v_0 \left( \frac{\partial u}{\partial y} + \frac{\partial w}{\partial y} \right) &= G_r \theta + G_c C + \frac{\partial^2 u}{\partial y^2} + \frac{\partial^2 w}{\partial y^2} - \\ \frac{M^2 \left( [(1 + \beta_m \beta_n)(u - 1) + \beta_m w] + [(1 + \beta_m \beta_n)w - \beta_m(u - 1)] \right)}{[(1 + \beta_m \beta_n)^2 + \beta_m^2]} & \end{aligned} \quad (3.51)$$

On applying the complex transformation explained above, equation (3.51) is therefore written as

$$\begin{aligned} \frac{\partial Z}{\partial t} - v_0 \frac{\partial Z}{\partial y} &= \frac{\partial^2 Z}{\partial y^2} + G_r \theta + G_c C - \\ \frac{M^2 \left( (1 + \beta_m \beta_n)(u + iw - 1) - i\beta_m(u + iw - 1) \right)}{[(1 + \beta_m \beta_n)^2 + \beta_m^2]} & \end{aligned} \quad (3.52)$$

or

$$\frac{\partial Z}{\partial t} - v_0 \frac{\partial Z}{\partial y} = \frac{\partial^2 Z}{\partial y^2} + G_r \theta + G_c C - \frac{M^2 \left( (1 + \beta_m \beta_n) - i\beta_m \right) Z}{[(1 + \beta_m \beta_n)^2 + \beta_m^2]} \quad (3.53)$$

Equation (3.45) after simplification becomes

$$\frac{\partial \theta}{\partial t} - v_0 \frac{\partial \theta}{\partial y} = \frac{1}{P_r} \frac{\partial^2 \theta}{\partial y^2} - \frac{B_i \theta}{P_r} + E_c \frac{\partial Z}{\partial y} \frac{\partial \bar{Z}}{\partial y} \quad (3.54)$$

The initial and boundary conditions after transformation become

For  $t \leq 0$ :

$$Z(y, 0) = 0, \theta(y, 0) = 0, C(y, 0) = 0 \quad (3.55)$$

For  $t > 0$  :

$$Z(0, t) = 1, \theta(0, t) = 1, C(0, t) = 1 \quad (3.56)$$

and

$$Z(\infty, t) = 0, \theta(\infty, t) = 0, C(\infty, t) = 0 \quad (3.57)$$

## CHAPTER 4

### MODEL SOLUTION

#### 4.1 Numerical technique:

It is a fact that unsteady partial differential equation models can only be solved numerically by finite difference techniques. In order to solve the unsteady non-linear partial differential equations (3.53), (3.54) together with (3.46) under the initial and boundary conditions in equations (3.55) to (3.57), a finite difference approximation scheme for the second derivative in space and first derivative in time has been employed. Equations (3.53), (3.54), and (3.46) in finite difference form are as follows, respectively.

$$\begin{aligned} \frac{Z_{i,j+1} - Z_{i,j}}{\Delta t} &= v_0 \frac{(Z_{i,j} - Z_{i-1,j})}{\Delta y} + \frac{(Z_{i-1,j} - 2Z_{i,j} + Z_{i+1,j})}{(\Delta y)^2} + \\ &G_r \theta_{i,j} + G_c C_{i,j} - \frac{M^2[(1 + \beta_m \beta_n) - i\beta_m]Z_{i,j}}{[(1 + \beta_m \beta_n)^2 + \beta_m^2]} \end{aligned} \quad (4.1)$$

$$\begin{aligned} \frac{\theta_{i,j+1} - \theta_{i,j}}{\Delta t} &= v_0 \frac{(\theta_{i,j} - \theta_{i-1,j})}{\Delta y} + \frac{(\theta_{i-1,j} - 2\theta_{i,j} + \theta_{i+1,j})}{P_r(\Delta y)^2} - \\ &\frac{B_i}{P_r} \theta_{i,j} + E_c \frac{(Z_{i,j} - Z_{i-1,j})}{\Delta y} \frac{(\bar{Z}_{i,j} - \bar{Z}_{i-1,j})}{\Delta y} \end{aligned} \quad (4.2)$$

$$\frac{C_{i,j+1} - C_{i,j}}{\Delta t} = v_0 \frac{(C_{i,j} - C_{i-1,j})}{\Delta y} + S_c \frac{(C_{i-1,j} - 2C_{i,j} + C_{i+1,j})}{(\Delta y)^2} \quad (4.3)$$

In this study, we used the approximate absolute value of the nodal point defined by  $(Z_{i,j} - Z_{i-1,j})(\bar{Z}_{i,j} - \bar{Z}_{i-1,j})$ , which is the numerator of last term in equation (4.2) as  $(Z_{i-1,j} - 2Z_{i,j} + Z_{i+1,j})$  as explained by Muschietti [37]. Using  $Z_{i,j} \equiv Z_i^j$ ,  $\theta_{i,j} \equiv \theta_i^j$ ,  $C_{i,j} \equiv C_i^j$ , equations (4.1), (4.2) and (4.3) in finite difference form can be explicitly written as follows:

$$Z_i^{j+1} = (a_i - v_0 d_i) Z_{i-1}^j + (v_0 d_i + 1 - 2a_i - M^2 \alpha_i) Z_i^j + a_i Z_{i+1}^j + \Delta t G_r \theta_i^j + \Delta t G_c C_i^j \quad (4.4)$$

$$\theta_i^{j+1} = \left(\frac{a_i}{P_r} - v_0 d_i\right)\theta_{i-1}^j + \left(1 + v_0 d_i - \frac{2a_i}{P_r} + \frac{B_i}{P_r}\Delta t\right)\theta_i^j + \frac{a_i}{P_r}\theta_{i+1}^j + E_c a_i (Z_{i-1}^j - 2Z_i^j + Z_{i+1}^j) \quad (4.5)$$

$$C_i^{j+1} = (a_i S_c - v_0 d_i)C_{i-1}^j + (v_0 d_i + 1 - 2a_i S_c)C_i^j + a_i S_c C_{i+1}^j \quad (4.6)$$

where

$$a_i = \frac{\Delta t}{(\Delta y)^2}, \quad d_i = \frac{\Delta t}{(\Delta y)}$$

and

$$\alpha_i = \frac{\Delta t(1 + \beta_m \beta_n) - i\beta_m}{(1 - \beta_m \beta_n)^2 + \beta_m^2}$$

The suffix  $i$  corresponds to nodal points in  $y$  while  $j$  corresponds to  $t$  (see Figure 4.1). Also  $\Delta t = t_{j+1} - t_j$  and  $\Delta y = y_{i+1} - y_i$ . Knowing the values of  $Z$ ,  $\theta$ , and  $C$  at a time  $t$ , we can then calculate their values at the next time step (see Figure 4.1). Although the boundary conditions for  $t > 0$  applies to  $y = \infty$ , (where  $\infty$  in this context refers to a large number). For convenience, we used domain length along the grid as  $y = 1.0$ . This choice of spacial length is applicable to modeling of MHD fluid flows over moving flat horizontal plates as explained by Makinde [22] and Kinyanjui [30] in their model solutions. We subdivided our solution domain on  $y$  into 101 solution points where  $i = 101$  as corresponding to  $y = \infty$  and therefore  $Z(101, j) = \theta(101, j) = C(101, j) = 0$ . This is chosen so because  $Z$ ,  $\theta$ ,  $C$  tend to zero at around  $y = 1.0$  as per the boundary equation (3.57).

The velocity at  $y = 0$ , ( $i = 0$ ) has to change rapidly to 1 from its value of zero at  $t < 0$  since the plate is impulsively set into motion by velocity  $U$ , hence  $Z_{0,j} = 1$ . The concentration of the injected material also changes rapidly to 1 from its zero value at  $t < 0$  giving  $C_{0,j} = 1$ .

While velocity and concentration change as explained, the temperature of the plate wall changes gradually due to the effect of the constant heat flux at the plate ( $y = 0$ ) hence  $\theta_{0,0} = 0$ . Therefore the following set of initial conditions are applied.

For  $t \leq 0$  : For all  $i$ :  $Z_{i,0} = 0$ ,  $\theta_{i,0} = 0$ ,  $C_{i,0} = 0$

The boundary conditions for the velocity, temperature and concentration are then given as follows:

For  $j > 0$  at  $y = 0$ :

$$Z_{0,j} = 1, \theta_{0,j} = 0, C_{0,j} = 1 \quad (4.7)$$

For  $j > 0$  at  $y = \infty$ :

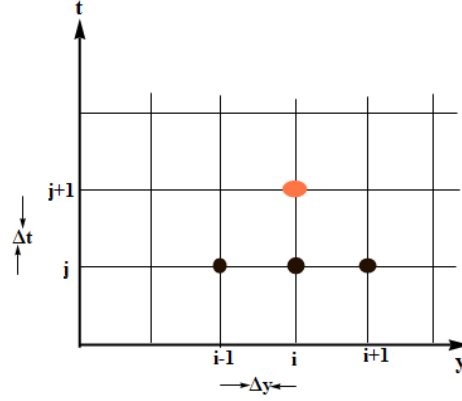


Figure 4.1: Computational molecule for the explicit numerical difference scheme.

$$Z_{\infty,j} =, \theta_{\infty,j} = 0, C_{\infty,j} = 0 \quad (4.8)$$

The difference equations (4.4) to (4.6) were programmed into a mathematica code (see Appendix). The velocity at the end of time step  $\Delta t$ , viz.  $Z(i, j+1)$ ,  $i = 1, 2, \dots, 100$  is computed from equation (4.4) in terms of velocities, temperatures and concentrations at points on earlier time step. Similarly,  $\theta(i, j+1)$  and  $C(i, j+1)$  are computed from equation (4.5) and (4.6) respectively. This procedure is continued until  $j = 1200$ . That is, up to time  $t = 0.048$ . Computations are carried out for water using  $P_r = 7.0$  as per the findings of Aziz [3]. The Grashof number,  $G_r = 0.2$  used corresponds to cooling of the plate by free convection. Other physical parameters used in the present study with their standard values when water is the fluid under consideration as explained by Aziz [3] and Crank [35] are:  $S_c = 0.4$ ,  $G_c = 1.0$ ,  $m^2 = 5.0$ ,  $E_c = 0.01$ ,  $v_0 = 0.5$ ,  $\beta_m = 1.0$ ,  $\beta_n = 0.2$  and  $B_i = 1.0$ .

## 4.2 Convergence and stability

A numerical method is said to be convergent if the solution of the difference equation by the numerical technique used tends to the exact solution of the difference equation as  $\Delta y$  and  $\Delta t$  both tend to zero. The difference between exact solution and numerical solution is called the discretization error. In general, the discretization error can be decreased by decreasing  $\Delta y$  and  $\Delta t$ . This means that the number of equations to be solved will increase and the method will be restricted by such

factors as time, degree of accuracy desired and computer core capacity.

A system of finite difference equations is stable when the cumulative effect of all the rounding errors is negligible. Since an explicit scheme of a finite difference technique is being used for determining the unknown nodal values at the  $(n + 1)^{th}$  time step from the nodal values at the  $n^{th}$  time step, there is need to know the largest time-step consistent with stability, for which the solution to the present problem is achievable.

In order to test convergence and stability, we used Von Neumann method for stability as explained by Crank [35], an explicit method is both convergent and stable if the mesh ratio parameter,  $\lambda$  is such that

$$\lambda = \frac{k' \Delta t}{(\Delta y)^2} \leq \frac{1}{2} \quad (4.9)$$

where  $k'$  in equation (4.9) is the coefficient of heat diffusivity.

Based on Crank's analysis on how to get a suitable mesh ratio for finite difference scheme for small heat flow rate, as in our case, he found out that  $k'$  can be taken to be  $1.0 \text{ cm}^2/\text{s}$ . To come up with the choice of step sizes for time and length, the following points were considered (based on the above discussion):

1. For finite difference method the control of accuracy and adjustment of the step size  $\Delta t$  is done by comparison of the results due to double or single step size. This is one of the many methods available in the literature as explained by Ram [23], Manyonge [36] and Makinde [22]
2. The explicit finite difference scheme satisfies the condition of stability given in equation (4.9)

For this case, in order to make sure that time-step,  $\Delta t$  is in line with stability criterion, we used spacial step size,  $\Delta y$  as 0.01 given that the grid length is 1.0 and grid range of 100 was chosen. The maximum time-step for this choice of  $\Delta y$  was 0.00005 corresponding to a mesh ratio of 0.5. The best results were obtained when we used 0.4 as the mesh ratio with  $\Delta t = 0.00004$  for the mathematica algorithm applied in the present study. The program was run with smaller values of time-step,  $\Delta t$  such as  $\Delta t = 0.00001$ ,  $0.000001$  and it was noted that there were no significant changes in the results, which ensures that the finite difference method used in this problem converges and is stable. That is, numerical solutions  $Z_i^j$ ,  $\theta_i^j$  and  $C_i^j$  of the discrete equations (4.4) to (4.6) approximate the analytical solutions  $Z(y, t)$ ,  $\theta(y, t)$  and  $C(y, t)$  respectively, of the p.d.e on the grid.

## CHAPTER 5

### RESULTS AND DISCUSSION

#### 5.1 Concentration profiles

To come up with results for the present research, numerical computations have been performed for the concentration, temperature and velocity. The results are represented by use of graphs.

The chemical species concentration profiles against span-wise coordinate  $y$  for varying values of physical parameters in the boundary layer flow can be analyzed from Figures 5.1-5.3. From these figures, it is seen that the concentration of the mass (chemical species) value of unity at the plate surface, remains fairly constant within the boundary layer but later on decreases rapidly till it attains the minimum value of zero far away from the plate surface. Physically, an increase in mass diffusion parameter,  $S_c$  means a decrease of molecular diffusion  $D$ . This could be happening because for higher values of  $S_c$ , there is a relatively reduced level of ion concentration in the fluid. Hence, the concentration of the species is higher for smaller values of  $S_c$  and lower for larger values of  $S_c$ . It is clear from Figure 5.1 that an increase in mass diffusion parameter,  $S_c$ , leads to a decrease in the concentration of the injected materials. However, the mass diffusion parameter is seen to have no effect on the concentration near the boundary. The effect of  $S_c$  is only noticed as the distance from the plate increases. Figure 5.2 reveals that the concentration of the injected materials increases with an increase in the time,  $t$  far away from the plate surface. This could be due to the cumulative concentration of the injected ions. Figure 5.3 shows that as the distance from the free stream region increases, the concentration profiles increase with the withdrawal of suction velocity,  $v_0$ .

#### 5.2 Temperature profiles

The influence of various thermophysical parameters on the temperature profiles against coordinate  $y$  is demonstrated in Figures 5.4-5.8. From Figure 5.4 it is noted that the temperature profiles increase with an increase in ion slip parameter,  $\beta_n$ . This can be attributed to the fact that temperature distribution depends upon the streams of the fluid and the velocity gradient of the fluid. In the present case, velocity changes with changes in  $\beta_n$  and Hall parameter,  $\beta_m$  in different proportions. The increase in  $\beta_n$  gives rise to increase in velocity resulting in increase

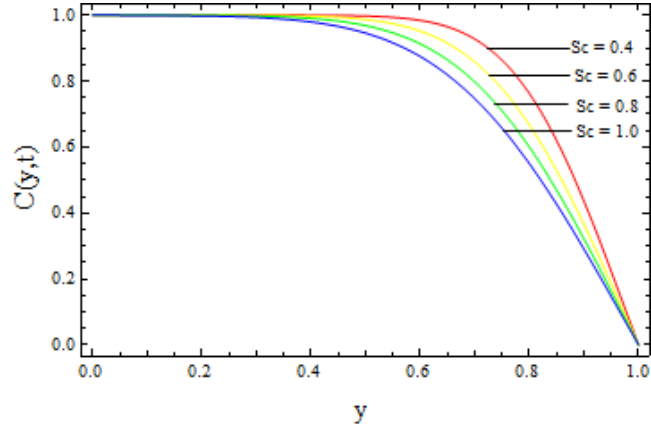


Figure 5.1: Concentration profiles for different values of  $S_c$  when  $v_0 = 0.5$  and  $t = 0.032$ .

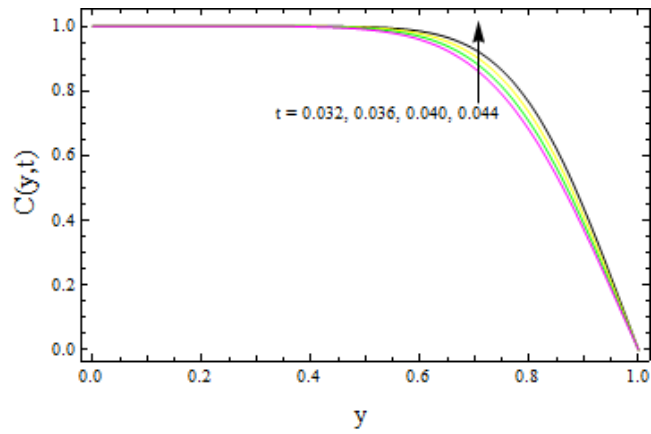


Figure 5.2: Concentration profiles for different values of  $t$  when  $S_c = 0.4$  and  $v_0 = 0.5$ .

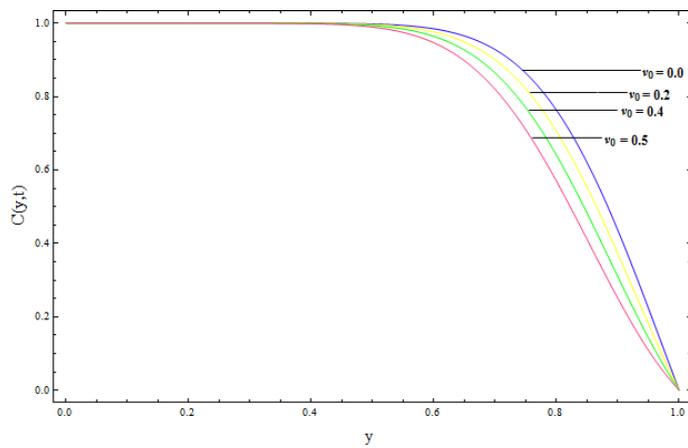


Figure 5.3: Concentration profiles for different values of  $v_0$  when  $S_c = 0.4$  and  $t = 0.32$ .

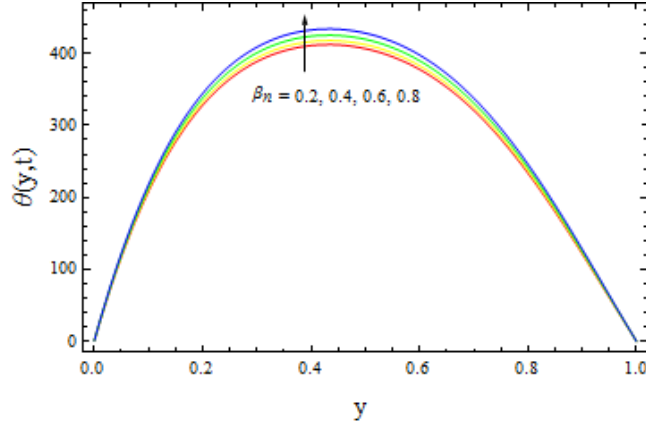


Figure 5.4: Temperature profiles for different values of  $\beta_n$  when  $S_c = 0.4$ ,  $v_0 = 0.5$ ,  $G_r = 0.2$ ,  $G_c = 1.0$ ,  $P_r = 7.0$ ,  $E_c = 0.01$ ,  $t = 0.032$ ,  $\beta_m = 1.0$ ,  $M^2 = 5.0$ ,  $B_i = 1.0$

in temperature while increase in  $\beta_m$  although increases velocity, it decreases the temperature fields within the flow. Figure 5.5 shows that an increase in modified Grashof number,  $G_c$  results in an increase in temperature profiles.  $G_c$  has an overall tendency to influence the velocity gradient of the flow hence increasing the velocity. This could be the reason for high temperatures when  $G_c$  is increased. It is observed from Figure 5.6 that an increase in Hall parameter,  $\beta_m$  leads to a decrease in the temperature profiles. It also seen from Figure 5.7 that an increase in time,  $t$  leads to a rise in temperature profiles of the fluid. This is because temperature increase as heat is continuously supplied to the fluid. Figure 5.8 reveals that the temperature profiles for the fluid is not affected by the withdrawal of the suction velocity,  $v_0$ . The reason is that the overall effect of  $v_0$  on velocity is seen to be zero hence no effect on temperature. It is observed in Figures 5.4-5.8 that at around mid-point,  $y = 0.5$  the temperature value is higher than the main source of heating which is the flat plate. The high temperatures ( $\theta \geq 100$ ) could be attributed to accumulation of heat within the flowing fluid as a result of heating by the plate, internal heat generation since the fluid is viscous and heat dissipation due to momentum diffusivity.

### 5.3 Velocity profiles

Figures 5.9 - 5.16 represent graphs of velocity distribution with span-wise coordinate  $y$  for different values of thermophysical parameters. It is evident from Figures 5.9, 5.10, 5.13 - 5.16 that for  $G_r > 0$ , velocity from its initial value of one at the plate surface increases gradually until it reaches its peak value away

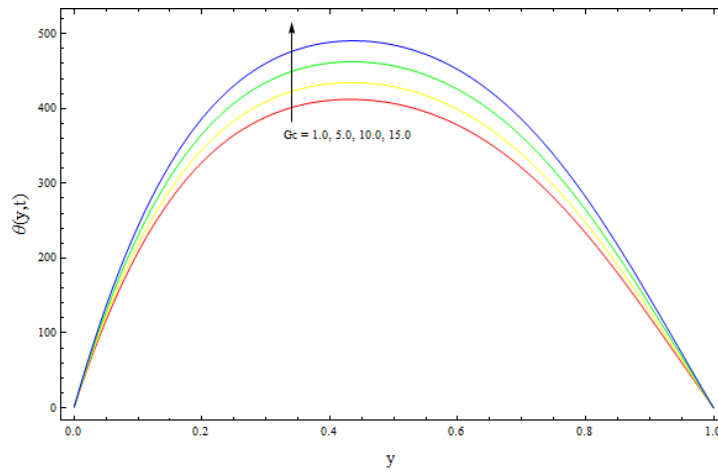


Figure 5.5: Temperature profiles for different values of  $G_c$  when  $S_c = 0.4$ ,  $v_0 = 0.5$ ,  $G_r = 0.2$ ,  $\beta_n = 0.2$ ,  $P_r = 7.0$ ,  $E_c = 0.01$ ,  $t = 0.032$ ,  $\beta_m = 1.0$ ,  $M^2 = 5.0$ ,  $B_i = 1.0$

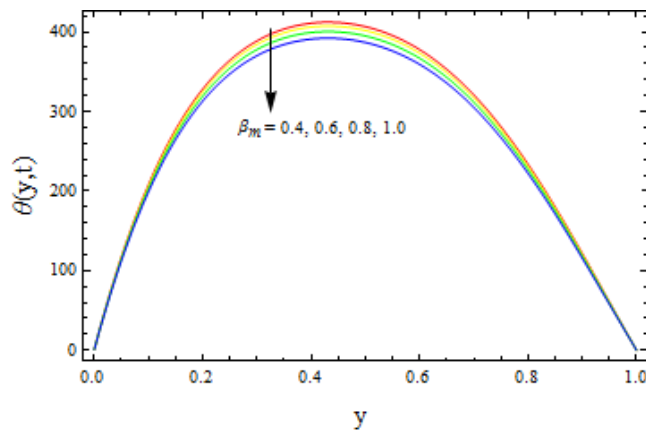


Figure 5.6: Temperature profiles for different values of  $\beta_m$  when  $S_c = 0.4$ ,  $v_0 = 0.5$ ,  $G_r = 0.2$ ,  $\beta_n = 0.2$ ,  $P_r = 7.0$ ,  $E_c = 0.01$ ,  $t = 0.032$ ,  $G_c = 1.0$ ,  $M^2 = 5.0$ ,  $B_i = 1.0$

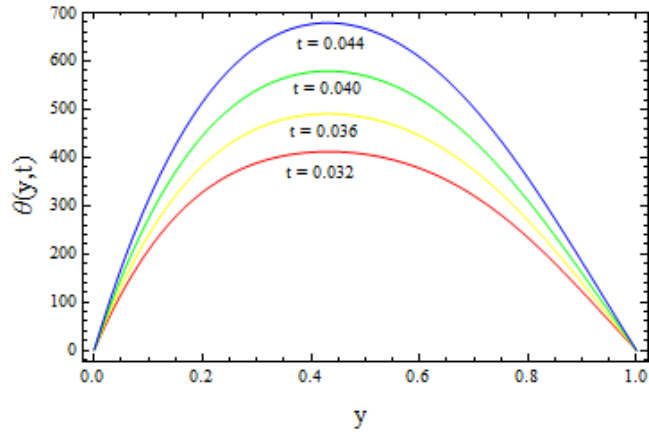


Figure 5.7: Temperature profiles for different values of  $t$  when  $S_c = 0.4$ ,  $v_0 = 0.5$ ,  $G_r = 0.2$ ,  $\beta_n = 0.2$ ,  $Pr = 7.0$ ,  $E_c = 0.01$ ,  $G_c = 1.0$ ,  $\beta_m = 1.0$ ,  $M^2 = 5.0$ ,  $B_i = 1.0$

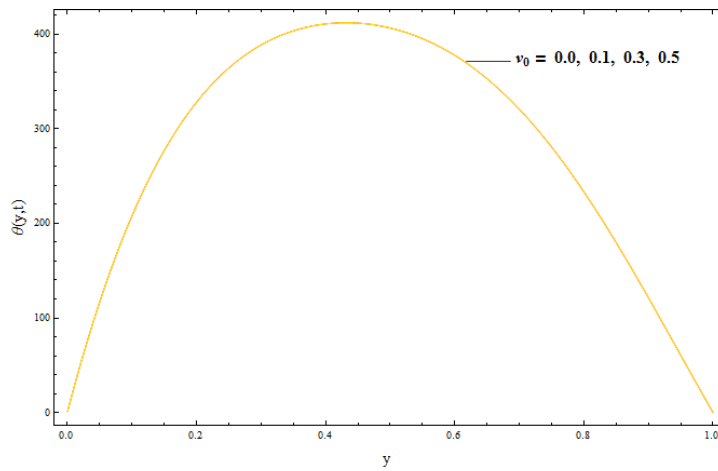


Figure 5.8: Temperature profiles for different values of  $v_0$  when  $S_c = 0.4$ ,  $G_c = 1.0$ ,  $G_r = 0.2$ ,  $\beta_n = 0.2$ ,  $Pr = 7.0$ ,  $E_c = 0.01$ ,  $t = 0.032$ ,  $\beta_m = 1.0$ ,  $M^2 = 5.0$ ,  $B_i = 1.0$

from the plate surface then gradually decreases to zero far away from the plate surface. For  $G_r < 0$ , (Figures 5.11 and 5.12) the velocity from its initial value of unity, drops to steady value approximately 0.2 near the boundary region before gradually attaining its minimum zero value far away from the plate surface. It is observed from Figure 5.9 that a decrease in Hall parameter,  $\beta_m$  leads to an a decrease in the velocity profiles. Figure 5.10 shows that velocity profiles rise with an increase in ion slip parameter,  $\beta_n$ . Figure 5.11 displays that for  $G_r = -0.2$ , the velocity profiles decrease as the Hall parameter,  $\beta_m$  falls. Figure 5.12 reveals that for  $G_r = -0.2$ , the velocity profiles increase as the ion slip parameter,  $\beta_n$  increases. The effects of  $\beta_n$  and  $\beta_m$  on velocity profiles can be explained that both parameters enhance the fluid velocity slightly, possibly due to the fact that the effective conductivity term,  $\left(\frac{\sigma}{(1+\beta_n\beta_m)^2+\beta_m^2}\right)$ , decreases with increase in  $\beta_n$  and  $\beta_m$  which decreases the magnetic resistance force hence increasing rate of fluid flow. It is noted from Figure 5.13 that an increase in squared magnetic parameter,  $M^2$  leads to a decrease in velocity profiles. This is attributed to the increasing damping force caused by presence of Lorentz force which decreases the fluid velocity. Figure 5.14 shows that an increase in modified Grashof number,  $G_c$  results in an increase in the velocity profiles. The possible reason for this observation being that the ionic strength of the fluid makes it more conductive hence creating more thermal force which increases the particles' speed. Figure 5.15 reveals that withdrawal of suction velocity,  $v_0$ , results in a decrease in the velocity from the plate surface to near the mid stream region but the velocity profiles rises as the distance increases past the free stream. This can be attributed to the fact that suction "delays" or prevents boundary layer separation since nearer the wall, the fluid travels at a lower velocity and also convection of the fluid pushes heated fluid past the mid-stream where the effect of boundary layer separation is more stable. It is observed from Figure 5.16 that an increase in time,  $t$  results in a large increase in the velocity profiles for the flow. This is mainly because the flow variables directly depend on time factor.

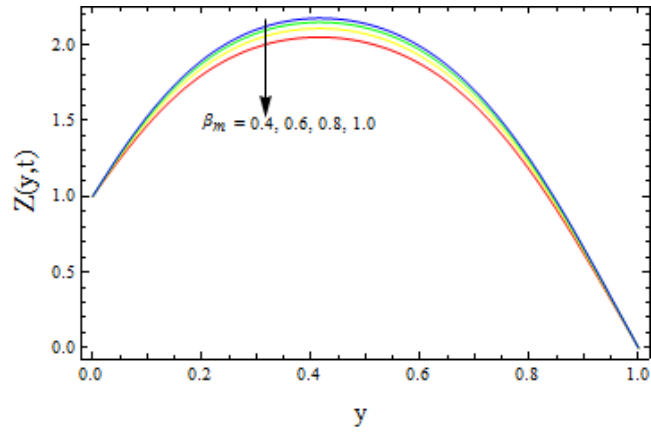


Figure 5.9: Velocity profiles for different values of  $\beta_m$  when  $S_c = 0.4$ ,  $v_0 = 0.5$ ,  $G_r = 0.2$ ,  $G_c = 1.0$ ,  $P_r = 7.0$ ,  $E_c = 0.01$ ,  $t = 0.032$ ,  $\beta_n = 0.2$ ,  $M^2 = 5.0$ ,  $B_i = 1.0$

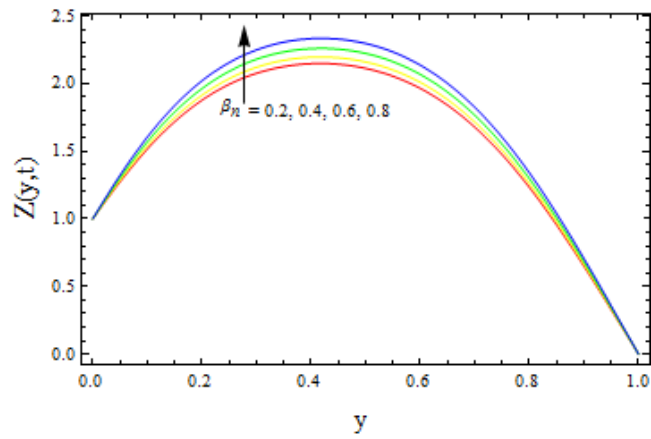


Figure 5.10: Velocity profiles for different values of  $\beta_n$  when  $S_c = 0.4$ ,  $v_0 = 0.5$ ,  $G_r = 0.2$ ,  $G_c = 1.0$ ,  $P_r = 7.0$ ,  $E_c = 0.01$ ,  $t = 0.032$ ,  $\beta_m = 1.0$ ,  $M^2 = 5.0$ ,  $B_i = 1.0$

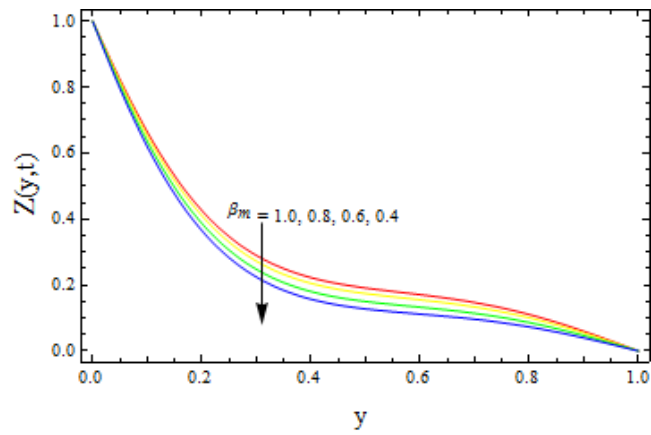


Figure 5.11: Velocity profiles for different values of  $\beta_m$  when  $S_c = 0.4$ ,  $v_0 = 0.5$ ,  $G_r = -0.2$ ,  $G_c = 1.0$ ,  $P_r = 7.0$ ,  $E_c = 0.01$ ,  $t = 0.032$ ,  $\beta_n = 0.2$ ,  $M^2 = 5.0$ ,  $B_i = 1.0$

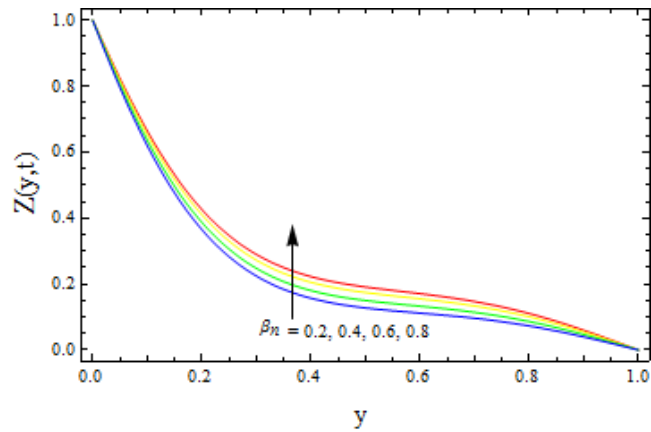


Figure 5.12: Velocity profiles for different values of  $\beta_n$  when  $S_c = 0.4$ ,  $v_0 = 0.5$ ,  $G_r = -0.2$ ,  $G_c = 1.0$ ,  $P_r = 7.0$ ,  $E_c = 0.01$ ,  $t = 0.032$ ,  $\beta_m = 1.0$ ,  $M^2 = 5.0$ ,  $B_i = 1.0$

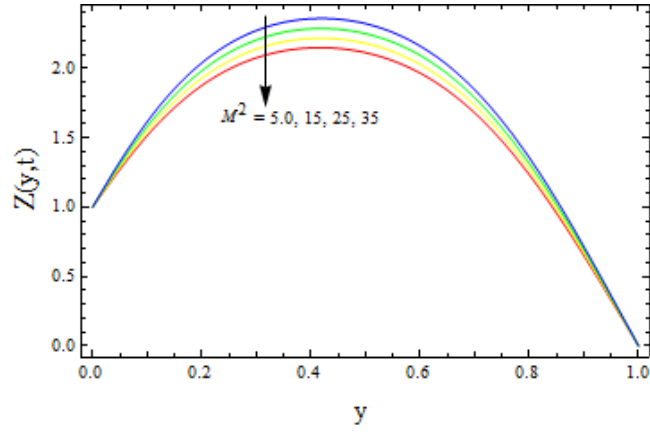


Figure 5.13: Velocity profiles for different values of  $M^2$  when  $S_c = 0.4$ ,  $v_0 = 0.5$ ,  $G_r = 0.2$ ,  $G_c = 1.0$ ,  $P_r = 7.0$ ,  $E_c = 0.01$ ,  $t = 0.032$ ,  $\beta_m = 1.0$ ,  $\beta_n = 0.2$ ,  $B_i = 1.0$

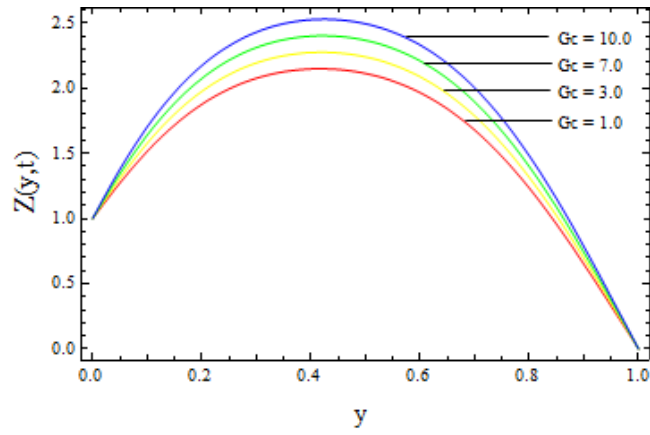


Figure 5.14: Velocity profiles for different values of  $G_c$  when  $S_c = 0.4$ ,  $v_0 = 0.5$ ,  $G_r = 0.2$ ,  $M^2 = 5.0$ ,  $P_r = 7.0$ ,  $E_c = 0.01$ ,  $t = 0.032$ ,  $\beta_m = 1.0$ ,  $\beta_n = 0.2$ ,  $B_i = 1.0$

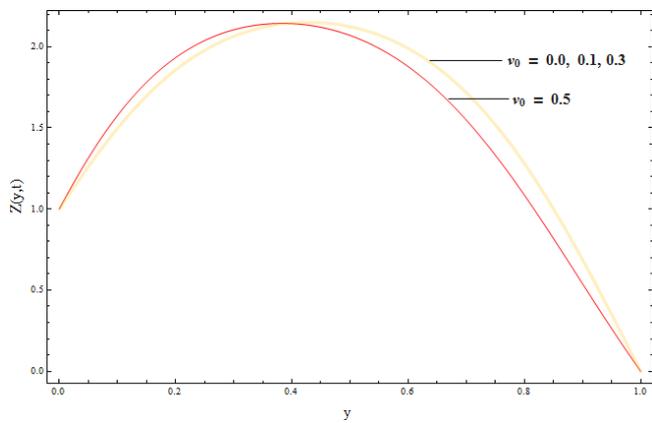


Figure 5.15: Velocity profiles for different values of  $v_0$  when  $S_c = 0.4$ ,  $G_c = 1.0$ ,  $G_r = 0.2$ ,  $M^2 = 5.0$ ,  $P_r = 7.0$ ,  $E_c = 0.01$ ,  $t = 0.032$ ,  $\beta_m = 1.0$ ,  $\beta_n = 0.2$ ,  $B_i = 1.0$

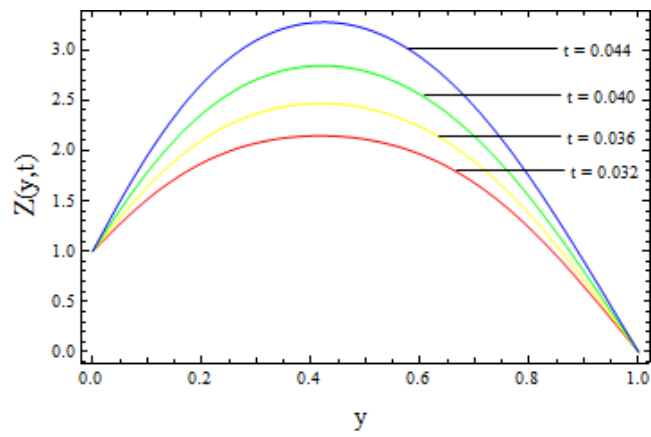


Figure 5.16: Velocity profiles for different values of  $t$  when  $S_c = 0.4$ ,  $G_c = 1.0$ ,  $G_r = 0.2$ ,  $M^2 = 5.0$ ,  $P_r = 7.0$ ,  $E_c = 0.01$ ,  $v_0 = 0.5$ ,  $\beta_m = 1.0$ ,  $\beta_n = 0.2$ ,  $B_i = 1.0$

## CHAPTER 6

### SUMMARY AND RECOMMENDATIONS

#### 6.1 Summary

In this work, we formulated governing MHD equations describing unsteady flow for a viscous, incompressible, electrically conducting fluid past an infinite flat plate subjected to mass and heat transfer with convective surface boundary condition. The resulting approximate coupled non-linear partial differential equations governing the flow after dimensionalization have been modeled numerically using explicit finite difference method. The final non-dimensionalized explicit difference equations were programmed into a mathematica code and the solutions were then generated. A parametric study of the specific parameters involved in the flow is conducted and a representative set of numerical results for the velocity and temperature distribution as well as concentration profiles are illustrated graphically to show trends of the solution to our research problem.

From the present numerical investigation, we established that for Prandtl number,  $Pr = 7.0$ , which corresponds to that of water, the temperature of the liquid generally increases from zero on the plate surface, attains a maximum value slightly away from the boundary region and then decreases to free stream value far away from the plate surface. This shows that in the presence of constant heat flux, cooling of the plate by free convection currents, ( $G_r > 0$ ) causes an increase in thermal boundary layer thickness. It was noticed that within the free stream region, the temperature value is higher than the main source of heating which is the flat plate. The high temperature could be as a result of accumulation of more heat within the flowing fluid caused by convective heating by the plate, internal heat generation since the fluid is viscous and heat dissipation due to momentum diffusivity.

For cooling of the plate by free convection currents ( $G_r > 0$ ) and presence of constant heat flux, an increase in ion-slip parameter and Hall parameter leads to an increase in velocity boundary layer thickness. This is because an increase in the two parameters have a general effect of suppressing heat conduction and magnetic resistance force thereby increasing flow velocity. However, for  $G_r < 0$ , which corresponds to heating of the plate by free convection currents and presence of constant heat flux, increase in ion-slip parameter and Hall parameter results in an increased velocity boundary layer thickness but of lower magnitude compared to those of  $G_r > 0$ . Reason being that as the plate is heated by convection, conductivity term is lowered more, magnetic resistance force is suppressed to a very low

value resulting into low velocity profiles.

For  $G_r > 0$ , it is observed that past the free stream region, increase in time produces an increase in concentration level while the concentration of the fluid decreases with increase in mass diffusion parameter,  $S_c$ . This is happening simply because for higher values of  $S_c$ , there is a relatively reduced level of ion concentration in the fluid. Also increase in time,  $t$  and  $G_c$  results in a thick boundary layer for both velocity and temperature as compared to the effects of other parameters. It is observed that using a strong magnetic field intensity, (increasing magnetic parameter,  $M^2$ ) degrades rather than enhance the momentum change efficiency. This is because the presence of magnetic field in an electrically conducting fluid introduces a force called Lorentz force, which acts against the flow if the magnetic field is applied in the normal direction to the flow, as in the present case. This type of resisting force slows down the fluid velocity. This finding on the effect of magnetic parameter is in agreement with what was observed by Kinyanjui et al [30] that an increase in magnetic parameter results in a decrease in the fluid velocity profiles.

An interesting finding in this study is the reversal nature of the effect of withdrawal of suction velocity,  $v_0$ , on the velocity. This reveals that without suction velocity, velocity of the fluid is lower on the plate surface than far away from the plate surface.

## 6.2 Recommendations

Finally, our analysis suggests several areas in which additional research would be useful. For example we recommend research on unsteady MHD heat and mass flow over a wavy plate for a turbulent flow with surface boundary condition.

We recommend that an extension of this study is pursued for a case where contribution of joule heating to the total heat energy (which we assumed to be negligible) is taken into consideration.

We do recommend also that an extension of this study is pursued for a case where the component of body forces along  $y_1$  (forces parallel to magnetic force field) is taken in consideration.

## REFERENCES

- [1] J. Hatman and F. Lazarus, *Experimental investigations on the flow of mercury in homogeneous magnetic field*, Reed Educational and Professional Publishing Ltd, (1937), 1-8.
- [2] H. Alfvén, *Existence of electromagnetic-hydrodynamic waves*, Nature, **150**, issue 3805, (1947), 405-406.
- [3] A. Aziz, *A similarity solution for laminar boundary layer over a flat plate with a convective surface boundary condition*, Communications in Nonlinear Science and Numerical Simulation, **14**, (2009), 1064-1068.
- [4] A.J. Chamkha, *Unsteady MHD convective heat and mass transfer past a semi-infinite vertical permeable moving plate with heat absorption*, International Journal of Engineering Science, **42**, (2004), 217-230.
- [5] A.K. Singh and N.C. Sacheti, *On hydromagnetic free-convection in the presence of induced magnetic field with constant heat flux*, International Journal of Science, **150**, (2010), 303-308.
- [6] G.E.A. Azzam, *Radiation effects on the MHD-Mixed free-forced convective flow past a semi-infinite moving vertical plate for a high temperature differences*, Journal of Physical science, **66**, (2002), 71-76.
- [7] B. Gebhart and J. Mollendorf, *Viscous dissipation in external natural convection flows*, Journal of Fluid Mechanics, **38**, (1969), 97-101.
- [8] H.S. Takha, A.K. Sing and G. Nath, *Unsteady MHD flow and heat transfer on a rotation disk in an ambient fluid*, International Journal of Thermal Science, **41**, (2002), 147-155.
- [9] K.A. Yih, *Free convective effect on MHD coupled heat and mass transfer of a moving permeable vertical surface*, International Communication of Heat and Mass Transfer, **26(1)**, (1999), 95-104.
- [10] E.M.A. Elbasheshy, *Heat and mass transfer along a vertical plate surface tension and concentration in the presence of magnetic field*, International Journal of Engineering Science, **34**, (1997), 515-522.
- [11] I. Pop and D.B. Ingham, *Convective heat transfer: Mathematical and computational modeling of viscous fluids and porous media*, Pergamon, Oxford university Press, (2001), 48-61.

- [12] V.M. Soundalgekar, S.K. Gupta and N.S. Birajdar, *Effects of mass transfer and free effect on NHD stokes problem for a vertical plate*, Nuclear Engineering Research, **53**, (1979), 309-316.
- [13] C.K. Dikshit and A.K Singh, *Hydrodynamic flow past a continuously moving semi-infinite plate for large suction*, Journal of Astrophysics and Space Science, **148**, (1988), 249.
- [14] A.Y. Ghaly, and M.A. Seddeek, *Chebyshev finite difference method for the effects of chemical reaction, heat and mass transfer on laminar flow along a semi-infinite horizontal plate with temperature dependent viscosity*, Chaos, Solitons and Fractals, (2004), 19-27.
- [15] O.D. Makinde and A. Ogulu, *The effect of thermal radiation on the heat and mass transfer flow of a variable viscosity fluid past a vertical porous plate permeated by a transverse magnetic field*, Chemical Engineering communication, **195(12)**, (2008), 1575-1584.
- [16] R.C. Bataller, *Radiation effects for the blasius and sakiadis flows with a convective surface boundary condition*, Applied Mathematics and computation, (2008), 832-840.
- [17] O.D. Makinde, *On MHD boundary layer flows and mass transfer past a vertical plate in a porous medium with constant heat flux*, International Journal of Numerical Method for Heat and Fluid Flow, **19(314)**, (2009), 546-554.
- [18] A. Postelnicu, *Influence of a magnetic field on heat and mass transfer by natural convection from vertical surfaces in porous media considering Soret and Dufour effects*, International Journal of Heat and Mass Transfer, **47**, (2004), 1467-1472.
- [19] R. Rajesuari, B. Jothiram and V.K. Nelson, *Chemical reaction, heat and mass transfer on non-linear MHD boundary layer flow through a vertical porous surface in the presence of suction*, Applied Mathematics and Science, **3(50)**, (2009), 2469-2480.
- [20] M.A. Seddeek, *Thermal radiation and buoyancy effects on MHD free convective heat generation flow over an accelerating permeable surface with temperature dependent viscosity*, Canadian Journal of Physics, **79**, (2001), 725-732.
- [21] R. Cortell, *Towards an understanding of the motion of mass transfer with chemically reactive species for two classes of viscoelastic fluid over a porous stretching sheet*, Chemical Engineering Process, **46**, (2007), 982-989.

- [22] O.D. Makinde, *On steady flow a reactive variable viscosity fluid in a cylindrical pipe with isothermal wall*, International Journal of Numerical Methods for Heat and Fluid flow, **17(2)**, (2007), 187-194.
- [23] P.C. Ram and C.B. Singh, *Unsteady magnetohydrodynamic fluid flow through a channel*, Journal of Science and Research, **28(2)**, (1978).
- [24] J.A. Shercliff, *Entry of conducting and non-conducting fluids in pipe*, Journal of Mathematical Proceedings of the Cambridge Philosophical Society, **52**, (1956), 573-580.
- [25] S. Ganesh and S. Krishnambal, *Unsteady MHD stokes flow of viscous fluid between two parallel porous plates*, Journal of Applied Science, **7**, (2007), 374-379.
- [26] M.A. Mansour, J.A. Hassanien and A.Y. Bakier, *The influence of lateral mass flux on free convection flow past a vertical flat plate embedded in a saturated porous medium*, Indian Journal of Pure and Applied Mathematics, **21(3)**, (1990) , 238-245.
- [27] P.C. Ram, M. Kinyanjui and H.S. Takhar, *MHD stokes problem of convective flow from a vertical infinite plate in a rotating fluid*, Journal of MHD Plasma Research, **5(2/3)**, (1995), 91-106.
- [28] V.G. Naidu, M.L. mittal and B.N. Rao, *Boundary layer heat transfer with electromagnetic fields*, Applied Mechanics Journal., **68(3/4)**, (1987), 277-286.
- [29] J.H. Merkin and T. Mahmood, *On the free convection boundary layer on a vertical plate with prescribed surface heat flux*, Journal of Inclusion Mathematics, **24(2)**, (1990), 95-107.
- [30] M. Kinyanjui, J.K. Kwanza and S. M. Uppal, *Magnetohydrodynamic free convection heat and mass transfer of a heat generating fluid past an impulsively started infinite vertical porous plate with hall current and radiation absorption* , Energy Conversion and Management, **42**, (2001), 919-922.
- [31] G.C. Dash and P.C. Tripathy, *Heat transfer in viscous flow a long a plane wall with periodic suction and heat sources*, Journal of Modelling Measurement and Control, **49(1)**, (1993), 18-22.
- [32] B.G. Sahoo and P.K. Sahoo, *Hydromagnetic free convection and mass transfer flow past an accelerated vertical plate through a porous medium*, Indian Journal of Technology, **24(9)**, (1986), 553-556.

- [33] A.O. Beg, A.Y. Bakier and V.R. Prasad, *Numerical study of free convection magnetohydrodynamic heat and mass transfer from a stretching surface to a saturated porous medium with Soret and Dufour effects*, Computational Materials and Science Journal, **46**, (2009), 57-65.
- [34] P. Chandra, *Fluid Mechanics*, Journal of Engineering, New Delhi India, (2005), 87-92.
- [35] J. Crank, and P. Nicolson, *A practical Method for Numerical Evaluation of solutions of practical differential equations of Heat conduction type*, Journal of Mathematical Proceedings of the Cambridge Philosophical Society, (**43**), (1947), 50-67.
- [36] A.W. Manyonge, *Elementary Fluid Mechanics*, A first Course, Lambert Academic Publishing, Saarbrucken, Germany, (2013).
- [37] L. Muschietti and C.T. Dum . *Real Group Velocity in a Medium with Dissipation*, Physics of Fluids B: Plasma Physics, **5(5)**, (1993), 1383.
- [38] A. Zangwill, *Modern Electrodynamics*, Cambridge University Press. ISBN 978-0-521-89697-9, (2013), 91-97.
- [39] A. Kumar, *Application of Runge-Kutta Method for the Solution of Non-Linear Pde*, UCD Publishers, Canada, (**26**), (1996), 2-6.
- [40] A.K. Singh and N.C. Sacheti, *Hydromagnetic free-convection flow with constant heat flux*, Journal of Astrophysics and Space Science, **150**, (1988), 303-308.

## APPENDICES

### A.1 Mathematica code (Concentration)

```
 $N_p = \text{"value"}; yI = \text{"value"}; yF = \text{"value"};$   
 $step = (yF - yI)/(N_p - 1); h = N[step];$   
 $S_c = \text{"value"}; u_0 = \text{"value"}; G_r = \text{"value"}; M^2 = \text{"value"};$   
 $B_i = \text{"value"}; P_r = \text{"value"}; E_c = \text{"value"}; \beta_m = \text{"value"};$   
 $\beta_n = \text{"value"}; \alpha = (1 - \beta_m * \beta_n - \beta_m)/((1 - \beta_m * \beta_n)^2 + \beta_m^2);$   
  
     $grid = Range[yI, yF, h];$   
     $np = Length[grid];$   
  
     $tstep = \text{"value"};$   
     $a1 = tstep * Map[(1/h - u_0)/h, , grid];$   
     $b1 = tstep * Map[(u_0 + h/tstep - m^2 * \alpha * h - 2/h)/h, , grid];$   
     $d1 = tstep * Map[1/h^2, , grid];$   
     $e = tstep * Map[G_r, grid];$   
  
     $f = tstep * Map[G_c, grid];$   
     $a2 = a1;$   
     $b2 = tstep * Map[(u_0 - (2/h) + h/tstep)/h, , grid];$   
     $d2 = d1;$   
     $a3 = tstep * Map[(S_c/h - u_0)/h, , grid];$   
     $b3 = tstep * Map[(u_0 - (2/h) * S_c + h/tstep)/h, , grid];$   
     $d3 = tstep * Map[S_c/h^2, , grid];$   
  
     $nsteps = \text{"value"};$   
     $v1 = Map[0, , grid]; v2 = Map[0, , grid]; v3 = Map[0, , grid];$   
     $Z = Map[1, , grid]; \theta = Map[1, , grid]; C = Map[1, , grid];$   
     $Z[[np]] = 0; \theta[[np]] = 0; C[[np]] = 0;$   
  
Do [{ $t = j * tstep;$ 
```

```

Do[{
    v1[[1]] = Z[[1]];
    v2[[1]] =  $\theta$ [[1]];
    v3[[1]] = C[[1]];
    v1[[np]] = Z[[np]];
    v2[[np]] =  $\theta$ [[np]];
    v3[[np]] = C[[np]];
    v1[[i]] = a1[[i]]Z[[i - 1]] + b1[[i]]Z[[i]] + d1[[i]]Z[[i + 1]]
              + e[[i]] $\theta$ [[i]] + f[[i]]c[[i]];

    v2[[i]] = a1[[i]] $\theta$ [[i - 1]] + b2[[i]] $\theta$ [[i]] + d1[[i]] $\theta$ [[i + 1]] - (Bi/Pr)
              *tstep + Ec * (Z[[i - 1]] - 2 * Z[[i]]) + (Z[[i + 1]]) * tstep/h2;
    v3[[i]] = a3[[i]]C[[i - 1]] + b3[[i]]C[[i]] + d3[[i]]C[[i + 1]], {i, 2, np - 1};

Z = Re(v1);
 $\theta$  = Re(v2);
C = v3;
If [Mod[j,"value"]==0, (Print[ListPlot[Transpose[{grid,C}], Frame → True, Joined
→ True,
Plotstyle → Red, FrameLabel → {Style["y", "value"], Style["C(y, t)", "value"]},
Epilog →
Style[Text["t = "<> ToString[t], {"value", 0.005}]]], {j, 1, nsteps}];

```

## A.2 Mathematica code (Temperature)

```

Np = "value"; yI = "value"; yF = "value";
step = (yF - yI)/(Np - 1); h = N[step];
Sc = "value"; u0 = "value"; Gr = "value"; M2 = "value";
Bi = "value"; Pr = "value"; Ec = "value"; beta_m = "value";
beta_n = "value"; alpha = (1 - beta_m * beta_n - beta_m)/((1 - beta_m * beta_n)^2 + beta_m^2);

  grid = Range[yI, yF, h];
  np = Length[grid];
  tstep = "value";
  a1 = tstep * Map[((1/h - u0)/h), , grid];
  b1 = tstep * Map[((u0 + h/tstep - m^2 * alpha * h - 2/h)/h), , grid];
  d1 = tstep * Map[(1/h^2), , grid];
  e = tstep * Map[Gr, grid];
  f = tstep * Map[Ec, grid];
  a2 = a1;
  b2 = tstep * Map[((u0 - (2/h) + h/tstep)/h), , grid];
  d2 = d1;
  a3 = tstep * Map[((Sc/h - u0)/h), , grid];
  b3 = tstep * Map[((u0 - (2/h) * Sc + h/tstep)/h), , grid];
  d3 = tstep * Map[Sc/h^2, , grid];

  nsteps = "value";
v1 = Map[0, , grid]; v2 = Map[0, , grid]; v3 = Map[0, , grid];
Z = Map[1, , grid]; theta = Map[1, , grid]; C = Map[1, , grid];
Z[[np]] = 0; theta[[np]] = 0; C[[np]] = 0;

Do [{t = j * tstep;

```

```

Do[{
  v1[[1]] = Z[[1]];
  v2[[1]] =  $\theta$ [[1]];
  v3[[1]] = C[[1]];
  v1[[np]] = Z[[np]];
  v2[[np]] =  $\theta$ [[np]];
  v3[[np]] = C[[np]];
  v1[[i]] = a1[[i]]Z[[i - 1]] + b1[[i]]Z[[i]] + d1[[i]]Z[[i + 1]]
    + e[[i]] $\theta$ [[i]] + f[[i]]c[[i]];
  v2[[i]] = a1[[i]] $\theta$ [[i - 1]] + b2[[i]] $\theta$ [[i]] + d1[[i]] $\theta$ [[i + 1]] - (Bi/Pr)
    *tstep + Ec * (Z[[i - 1]] - 2 * Z[[i]]) + (Z[[i + 1]]) * tstep/h2;
  v3[[i]] = a3[[i]]C[[i - 1]] + b3[[i]]C[[i]] + d3[[i]]C[[i + 1]], {i, 2, np - 1}];

```

```
Z = Re(v1);
```

```
 $\theta$  = Re(v2);
```

```
C = v3;
```

```
If [Mod[j,"value"]==0, (Print[ListPlot[Transpose[{grid, $\theta$ ]], Frame  $\rightarrow$  True, Joined
 $\rightarrow$  True,
```

```
Plotstyle  $\rightarrow$  Red, FrameLabel  $\rightarrow$  {Style["y", "value"], Style[" $\theta$ (y, t)", "value"]},
```

```
Epilog  $\rightarrow$ 
```

```
Style[Text["t = "<> ToString[t], {"value", 0.005}]]], {j, 1, nsteps}];
```

### A.3 Mathematica code (Velocity)

```

Np = "value"; yI = "value"; yF = "value";
step = (xF - xI)/(Np - 1); h = N[step];
Sc = "value"; u0 = "value"; Gr = "value"; M2 = "value";
Bi = "value"; Pr = "value"; Ec = "value"; beta_m = "value";
beta_n = "value"; alpha = (1 - beta_m * beta_n - beta_m)/((1 - beta_m * beta_n)^2 + beta_m^2);

grid = Range[yI, yF, h];
np = Length[grid];
tstep = "value";
a1 = tstep * Map[((1/h - u0)/h), , grid];
b1 = tstep * Map[((u0 + h/tstep - m^2 * alpha * h - 2/h)/h), , grid];
d1 = tstep * Map[(1/h^2), , grid];
e = tstep * Map[Gr, grid];
f = tstep * Map[Ec, grid];
a2 = a1;
b2 = tstep * Map[((u0 - (2/h) + h/tstep)/h), , grid];
d2 = d1;
a3 = tstep * Map[((Sc/h - u0)/h), , grid];
b3 = tstep * Map[((u0 - (2/h) * Sc + h/tstep)/h), , grid];
d3 = tstep * Map[Sc/h^2, , grid];

nsteps = "value";
v1 = Map[0, , grid]; v2 = Map[0, , grid]; v3 = Map[0, , grid];
Z = Map[1, , grid]; theta = Map[1, , grid]; C = Map[1, , grid];
Z[[np]] = 0; theta[[np]] = 0; C[[np]] = 0;

Do [{t = j * tstep;

```

```

Do[{
  v1[[1]] = Z[[1]];
  v2[[1]] =  $\theta$ [[1]];
  v3[[1]] = C[[1]];
  v1[[np]] = Z[[np]];
  v2[[np]] =  $\theta$ [[np]];
  v3[[np]] = C[[np]];
  v1[[i]] = a1[[i]]Z[[i - 1]] + b1[[i]]Z[[i]] + d1[[i]]Z[[i + 1]]
    + e[[i]] $\theta$ [[i]] + f[[i]]c[[i]];
  v2[[i]] = a1[[i]] $\theta$ [[i - 1]] + b2[[i]] $\theta$ [[i]] + d1[[i]] $\theta$ [[i + 1]] - (Bi/Pr)
    *tstep + Ec * (Z[[i - 1]] - 2 * Z[[i]]) + (Z[[i + 1]]) * tstep/h2;
  v3[[i]] = a3[[i]]C[[i - 1]] + b3[[i]]C[[i]] + d3[[i]]C[[i + 1]], {i, 2, np - 1}];

```

```
Z = Re(v1);
```

```
 $\theta$  = Re(v2);
```

```
C = v3;
```

```
If [Mod[j,"value"]==0, (Print[ListPlot[Transpose[{grid,Z}], Frame → True, Joined
→ True,
```

```
Plotstyle → Red, FrameLabel → {Style["y", "value"], Style["Z(y, t)", "value"]},
```

```
Epilog →
```

```
Style[Text["t = "<> ToString[t], {"value", 0.005}]]], {j, 1, nsteps}];
```